Investigation of Temperature effects on Electro Mechanically cooled Ge Detectors

Clara Hannigan

Masters By Research

University of York
Department of Physics
Nuclear Physics Group

April 30, 2010

Contents

Acknowledgements

Firstly, I would to thank my supervisor Professor Bob Wadsworth for all his help and guidance over the duration of this thesis project. I would also like to acknowledge Sellafield Ltd. whom without their finanical support this project would not have been possible. In particular, Robert Glover from Sellafield was deeply involved in this project from the outset and I would like to thank him for his useful input throughout. The technical staff in the University of York were always there to lend a hand whenever they were needed, especially Dave Coulthard, Richard Armitage and Neil Johnson, who were responsible for the construction of the temperature controlled enclosure. This project was only made possible by the co-operation of Ortec and Canberra Eurisys and therefore I would like to thank them for their generous loans of the detectors used in this project. Also, I would also like to express my appreciation to all in the Nanocentre at the University of York for allowing me to use their clean room for the duration of the project. Finally, I would like to thank my family, housemates and colleagues for all their help and support over the duration of this project.

Abstract

The motivation for this project originated due to anecdotal evidence that Ge detectors encountered problems with energy resolution when they were located in uncontrolled environmental conditions, in which temperature variations can be as great as 30°C. This project aims to investigate how much of an effect this temperature variation has on the resolution of the detectors and if so to what extent. Three Ge detectors were used in this project, an Ortec electro mechanically cooled Xcooler detector, an Ortec liquid nitrogen cooled detector and a Canberra cryo-cycle hybrid electro mechanical/liquid nitrogen cooled detector. The ambient room temperature was controlled between temperatures of $\sim$ 5 - 30^{o}C and the energy resolution for the 60, 122, 779 and 1408 keV gamma peaks was determined for each of the three detectors at both low (1000counts/sec) and high (20,000counts/sec) count rates. Plots of normalised resolution versus ambient room temperature were analysed. The results for the Ortec Xcooler detector concluded that there was no significant change in resolution within error for low count rate data, however, there was evidence for a small but statistically significant change in resolution of the high energy gamma rays at high count rates. The Canberra Cryocycle detector showed a significant improvement in resolution for the low energy gamma peaks at low count rates, with some weak evidence suggesting that the resolution of the low energy gamma rays of the high count rate data may follow a similar trend. Finally, the Ortec Liquid Nitrogen cooled detector did not display any significant changes in resolution within errors at both low and high count rates. Further verification is necessary to confirm these results but the Ortec Xcooler detector and the Canberra Cryocycle detector both exhibit preliminary results that support the anecdotal evidence put forward by Sellafield, however, in the case of the Ortec Liquid Nitrogen cooled detector, this anecdotal evidence was unfounded.

Declaration

I declare that the work presented in this thesis, except where otherwise stated, is based on my own research and has not been submitted previously for a degree in this or any other university.

Signed

Clara Hannigan

Chapter 1

Introduction

Section 1.1 of this chapter outlines the motivation behind the project, while section 1.2 highlights the prime goals to be achieved. Section 1.3 discusses some of the implications and benefits of this research to Sellafield, while section 1.4 provides some basic background theory in relation to Ge detectors and some of their properties.

1.1 Motivation

Germanium detectors have been the detector of choice for many years especially in gamma-ray spectroscopy because they offer excellent energy resolution, for a wide range of energies from a few keV up to 10 MeV. However this advantage is offset by the need to maintain these detectors at low temperatures usually using Liquid Nitrogen (77K) while operating under high voltage. This requirement is inconvenient in some situations because it may require the nitrogen dewar to be filled more than once a week. An alternative to cooling with Liquid Nitrogen has been developed in which refrigeration methods have been used. Two electro-mechanically cooled germanium detectors are used in this project. The prime purpose of this project was to test a variety of Ge detectors to investigate if the energy resolution of selected low and high energy gamma ray lines varied as a function of the ambient temperature in which the detector is located, and, if possible, to check if the crystal temperature, and hence the resolution, varied with ambient room temperature. This project arose because of the anecdotal evidence that were problems for detectors that are used to try and monitor particular gamma-rays when they are located in uncontrolled environmental conditions in Sellafield. Such detectors can be subject to significant temperature variations, which may be as large as 30^{o}C. The project aims to test whether this temperature variation has an effect on the resolution of these detectors and if so to what extent. Such variations can impact on the ability of software to monitor radiation from nuclides.

1.2 Prime goals of the Project

Initially it was expected that up to seven detectors may be involved in the tests. However due to delivery problems three Germanium detectors were eventually used in this project; two electro-mechanically cooled detectors (one of which was a hybrid electro mechanical/liquid nitrogen cooled detector) and a liquid nitrogen cooled detector. Canberra Eurysis and Ortec supplied these detectors. All tests were investigated for a range of gamma ray energies (60 keV to 1.4 MeV) under controlled environmental conditions. There were five main aims in this project. The prime aim was to measure the change in resolution for a range of gamma energies as a function of ambient temperatures for both low and high count rates. A further goal was to measure this as a function of crystal temperature, if possible via the use of the PT1000 signal. Another objective was to investigate if varying the temperature of the room in which the electronics used to process signals from the detectors were housed would have an effect on the resolution of the selected gamma peaks. Since the cooler can be turned off on the Canberra cryo-cycle hybrid detector, an investigation was carried out to see if the electric cooler has an impact on the resolution of the selected gamma peaks. Finally the absolute detector efficiencies were measured using a ^{60}Co source. The key energy range of interest to Sellafield was 50 – 150 keV (because the detector response is exacerbated in this energy range) but it agreed that a broader energy range would be analysed in this project: from $\sim$ 60 keV up to 1408 keV. ^{241}Am and ^{152}Eu were selected to achieve this energy range, both with an activity of $\leq$ 370 kBq.

1.3 Implications and Benefits of this Research

The study of temperature effects on resolution was of interest to Sellafield in order to establish if extreme changes in environmental temperature would have a significant effect on the resolution, and if so to quantify these changes. The study using the Canberra Cryocycle detector (pump on and pump off) set out to establish if the electronic noise associated with the cooling system would result in a broader resolution. This electronic noise should only add some random element to the signal causing a broader peak. The data obtained during these tests will be used to support the substantiation of using electro-cooled detectors. These tests will help convince future system designers at Sellafield that by using electro-mechanically cooled detectors, that they can get similar performance while reducing the health and safety concerns associated with the

liquid nitrogen cooling methods. However, any modifications made to the existing systems would follow a rigourous substantiation process involving proper testing and partial re-commissioning, rather than being solely based on the findings of this thesis. The final results of this thesis will help make decisions at Sellafield rather than directly affect the existing systems.

1.4 Background Theory

1.4.1 Ge Detector

A Germanium Detector is comprised of a single crystal of Germanium. When the energy from ionizing radiation is transferred to the Ge crystal, electron-hole pairs are created. Under reverse bias (normal operating) conditions, the electrons in the conduction band move in one direction while the holes in the valence band move in the opposite direction. This movement of electrons and holes in the semiconductor crystal creates a current, and the amplitude of the resulting pulse is proportional to the energy deposited in the crystal by the incoming ionizing radiation. The current generated is passed to a charge sensitive preamp which is used to generate an output voltage pulse [Kno00a]. In order to reduce the trapping and recombination of the electrons and holes, high purity Germanium is used. Detectors that use this high purity germanium are referred to as intrinsic or high-purity (HPGe) detectors. Fabrication techniques can achieve impurity levels as low as 10^9atoms/cm^3. Low level impurities may remain, if they are electron acceptors, the crystal will be mildly p-type whereas, if these impurities are electron donors, the crystal will be mildly n-type [Kno00b].

Ge detectors operate under a specified high voltage (3000-4000V for Ge detectors). The higher the external voltage applied the larger the depletion region becomes and thus the larger the sensitive volume will be for radiation detection. The maximum voltage applied depends on the resistance, whereby the junction will breakdown and begin conducting [Leo94a]. This maximum high voltage will be specified by the manufacturer. When a Ge detector is operated under the specified high voltage, it must be maintained at a temperature of $\sim$ 77k (liquid nitrogen) to reduce leakage current and ensure that it can provide optimal resolution performance [Kra88a].

There are many different types of detectors available. The basic construction for the three used in this project is described in more detail in section 1.4.2.

1.4.2 HPGE Coaxial and BEGE Detectors

High Puirty GE Coaxial Detectors

A cylindrical crystal of p-type Ge material is used and the core of the crystal is removed. An n+ contact is attached to the outer surface, with a p+ contact placed on the inner walls of the removed core. Since the crystal can be made long in the axial direction, the active volume of the detector crystal is increased [Kno00c]. The Ortec x-cooler detector used this p-type configuration (see Figure 1.1(a)). The liquid Nitrogen cooled detector from Ortec has an n-type configuration in which a cylindrical crystal of n-type Germanium material is used. But in this case the p+ contact is attached to the outer surface with the n+ contact fabricated on the inner walls.(see Figure 1.1 (b))

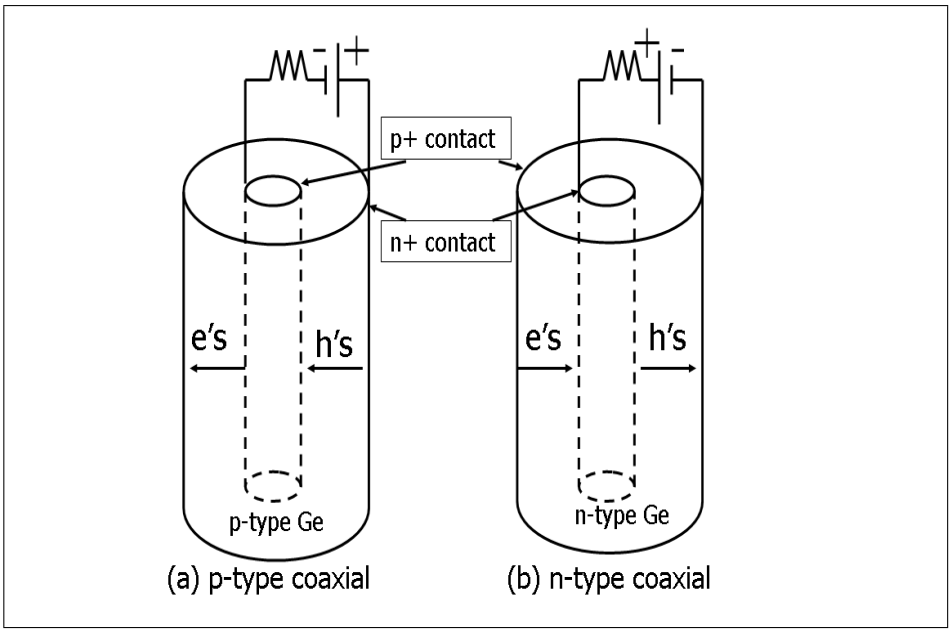

Figure 1.1: Schematic figure showing p-type (a) and n-type (b) coaxial configurations for Ge detectors. The electrons and holes are given by e's and h's respectively, while the arrows indicate the direction of flow of charge in each case. The typical dimensions of a coaxial crystal are as follows: diameter of crystal 81.9mm and the length of the crystal 52.5mm (ortec x-cooler detector).

The p+ contact is thicker than the n+ contact. If the thicker contact is on the outside, then there is a loss in detector efficiency at low gamma-ray energies because this is effectively a dead layer. The much thinner n+ contact does not absorb radiation as much as the p+ contact does. Therefore the n-type semiconductor has the advantage that its sensitivity can extend to below 10 keV [Leo94b].

Broad Energy GE Detectors

The detector supplied by Canberra was a BEGE (Broad Energy Ge) detector. This detector covers the energy range of 3 keV up to 3 MeV (as quoted by manufacturers). The shape of the BEGE crystal is short and fat, which offers a large area of sensitivity (see Figure 1.2). This improves efficiency below 1 MeV for typical geometries [Can03]. Small volume detectors have a significant advantage over large volume detectors for making energy resolution measurement for two main reasons; The first is that the electronic noise of a system increases with detector capacitance and smaller detectors have lower capacitances compared with larger detectors. The second factor reflects the increased carrier loss experienced due to trapping in large volume detectors because of the larger distances travelled by the charge carriers in these detectors compared with the small volume detectors [Kno00d]. The electrode structure of the BEGE is optimum for resolution at low energy and the crystal is fabricated from germanium that has an impurity profile that improves charge collection at the higher energies of the spectrum. Therefore, the BEGE displays high energy resolution at both low and high energies, thus covering an extensive energy range [Can03].

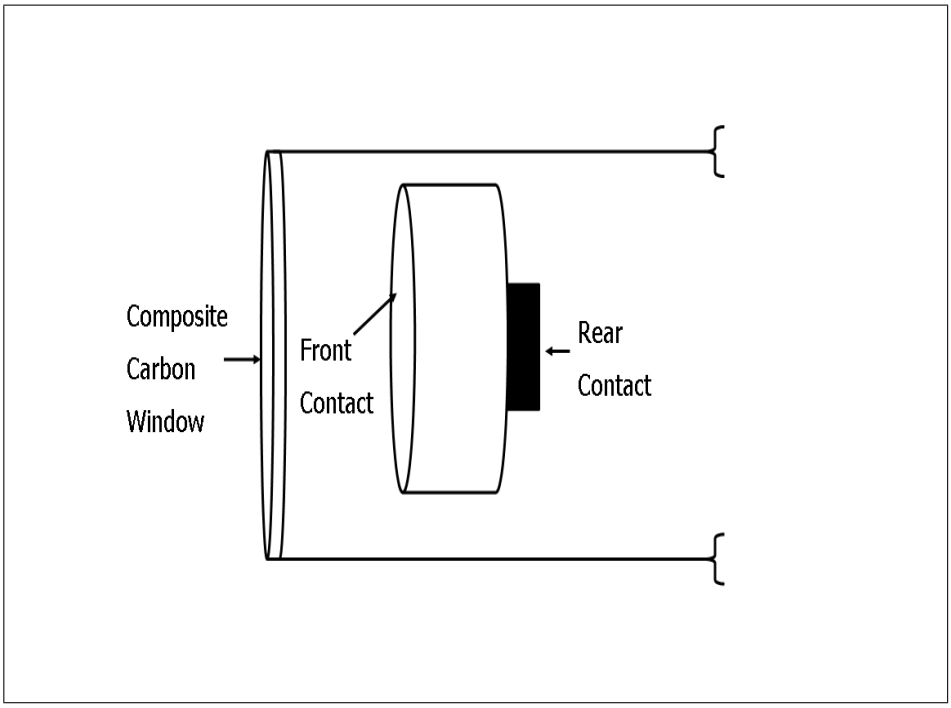

Figure 1.2: Schematic diagram illustrating the configuration of a BEGE detector. The dimensions of the BEGE detector are as follows: diameter of the crystal is 70mm and thickness of the crystal is 25mm (Canberra cryocycle detector).

1.4.3 Resolution

The main application of Ge Detectors is in high-resolution gamma-ray spectroscopy (0.17% at 1332 keV [Kra88b]). Virtually all gamma ray spectroscopy is carried out using these detectors because of their ability to resolve many close lying gamma ray energies, which would remain unresolved in other detector systems such as a NaI scintillator.

The energy resolution of a Ge system is determined by a combination of three factors. The first is the inherent statistical spread in the number of charge carriers (W_D). The next factor is due to the variations in the charge collection efficiency (W_X) and the final factor is the contribution of electronic noise (W_E) [Kno00d]. The spectrum consists of gamma peaks that are of finite width (which results primarily from the statistical variations in the number of electron-hole pairs produced for a given photon energy (W_D) and are typically Gaussian in shape [Leo94c].

The observed resolution is usually quoted in terms of Full Width at Half Maximum, W_T, (FWHM) of the peak and can be expressed as follows:

$$W_{T^2} = W_{D^2} + W_{X^2} + W_{E^2}, \tag{1.1}$$

where $W_D{}^2$ is given by

$$W_{D^2} = (2.35)^2 \times F \times \epsilon \times E, \tag{1.2}$$

where

F = The Fano Factor,

ϵ = Energy necessary to create electron-hole (e-h) pairs ($\sim$ 3 eV in Ge),

and E = Gamma ray energy.

The factor 2.35 relates the standard deviation of a Gaussian to its FWHM.

The Fano factor is a function of the fundamental processes that lead to an energy transfer in the crystal of the detector. F $\sim$ 0.05 for semiconductor detectors such as Ge [Leo94c].

$W_X{}^2$ represents incomplete charge collection and is important in large volume detectors [Kno00d]. $W_E{}^2$ corresponds to broadening effects of the electronics in the system once the signal leaves the detector, such as the preamplifier and the amplifier [Kno00d]. For a HPGe detector, the $W_X{}^2$ and $W_E{}^2$ terms will have more of an influence at low energies while degradation in the resolution due to $W_D{}^2$ becomes evident at higher energies [Kno00d]. Examining equation (1.2) in further detail, we can see that the resolution is a function of the energy deposited in the crystal since W_D is dependent on E.

Therefore,

$$W_T \propto E^{1/2}. \tag{1.3}$$

Resolution is generally measured by examining spectra taken using a detector. Figure 1.3 illustrates the FWHM, W_T of the peak.

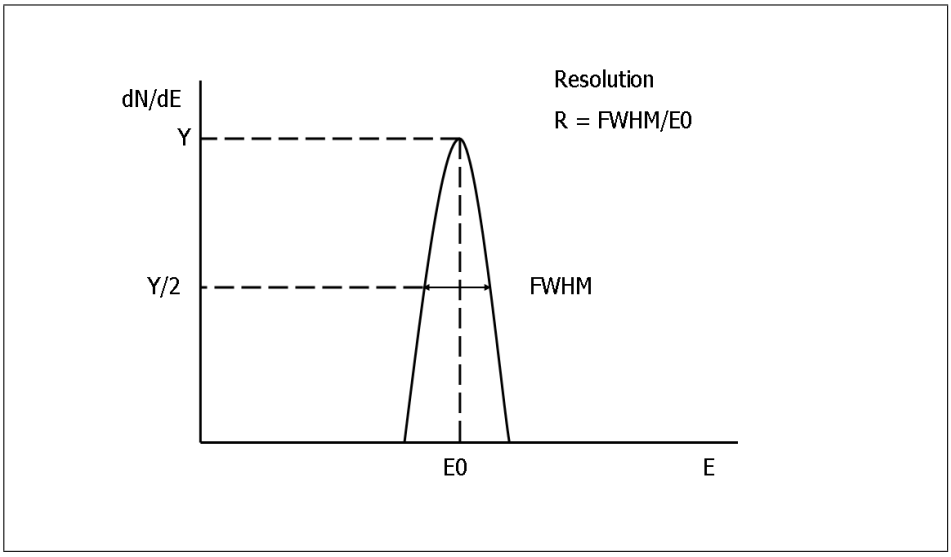

Figure 1.3: Schematic illustrating Resolution and FWHM of a given peak of finite width.

1.4.4 Efficiency of a Ge Detector

Absolute Efficiency

The absolute efficiencies of the three detectors used in this project were determined. The absolute efficiency is measured using the following method: firstly a ^{60}Co source is placed 25 cm from the crystal face (distance from end cap to crystal face needs to be taken into account) along the axis of the cylinder. A spectrum of the ^{60}Co source is then collected. The absolute detector efficiency ($\varepsilon_{absolute}$) is defined as the ratio of counts in the 1333 keV peak per unit time divided by the activity of the ^{60}Co source [Kno00e].

I.e.,

$$\varepsilon_{absolute} = \frac{\text{Number of counts in the 1333 keV peak/Unit time}}{\text{Activity of the source}}. \tag{1.4}$$

Some detector geometries are complex and the absolute efficiency is difficult to determine from the observed count rate due to uncertainties in the effective detector solid angle. To eliminate this problem manufacturers often use a relative efficiency ($\varepsilon_{relative}$) to quote detector efficiency [Kno00e].

Relative Efficiency

The manufacturers of the Ge detectors used in this project have quoted the efficiency of the detectors relative to a 3 inch by 3 inch NaI scintillator crystal at a specific energy (i.e. The 1333 keV peak from the ^{60}Co source) and distance (25 cm) from the crystal. The absolute efficiency is determined using the method described above.
$\varepsilon_{absoluteNaI}$ for a NaI scintillator at 25 cm for the 1333 keV peak is given by 1.2 $\times 10^{-3}$ [Kno00e]. The ratio of these two figures is quoted as the relative efficiency of the detectors used in this project [Kno00e].

$$\varepsilon_{relative} = \frac{\varepsilon_{absoluteGe}}{\varepsilon_{absoluteNaI}}. \tag{1.5}$$

Chapter 2

Experimental Details

This chapter outlines the experimental preparation done during the initial stages of the project in order to have a final experimental set-up ready for when the first detector arrived. Section 2.1 discusses the various options that were available to us to house the electronics for the experiment. Section 2.2 discusses the tests carried out which lead us to a pretested set of BNC and SHV cables and NIM modules which were reserved for the all detectors. Section 2.3 and 2.4 introduces the temperature data loggers and MCA respectively, that were used over the duration of the project. Section 2.5 discusses the work that went into designing and building a temperature controlled environment. Section 2.6 describes the range of tests carried out to determine the temperature stability of this enclosure. Finally, section 2.7 presents some of the final parameters used in the project. Section 2.7.1 discusses the energy range of interest and the sources selected that cover this range. The temperature range of interest is presented in section 2.7.2. The count rate and shaping time for both the low and high count rate is examined in section 2.7.3. Finally, the data acquisition time is reviewed in section 2.7.4.

2.1 Temperature stability of Electronics

Consideration was given as to the best possible method to ensure that the temperature of the electronics (i.e. the nuclear instrumentation units (NIM) used to process the signals) was kept constant whilst the Ge operating condition temperature was varied. One option was to build a separate box to place the electronics in, but it was felt not to be a viable option because of the heating effects of the NIM bin and the electronic modules themselves. The alternative to this was to use the temperature controlled

clean room, which was located in the Nanocentre in the University of York. This room, which is large (and empty at the time of use) and has, in principle, a temperature stability of $\pm$ 0.2 ^{o}C was felt to provide a much better environment for the electronics.

2.2 Stability of NIM Units

At the outset, much time was spent investigating issues that needed to be factored into the final experimental setup. In order to carry out these preliminary tests, an Ortec liquid nitrogen Germanium detector from the University of York was used. These tests were carried out using an Ortec 8k ADC and Maestro DAQ system [Ortc]. This detector was used in conjunction with an Ortec 659 model bias supply and a 572-spectroscopy amplifier. The key focus of these tests was to assess the stability of the electronics to be used in final experimental setup in the Nanocentre. Once the factors affecting the stability of the system had been determined, these were then factored into future work and adjustments were made where appropriate. Once a set of NIM units was found to give the best stability for the system, these were reserved for all future tests. The only exception to this rule was with regards to compatibility issues with the detector and the NIM units, for example the high voltage shut down signal for the Canberra detector needed a specific high voltage power supply, which was loaned to us by the manufacturer.

Investigating the stability of the system involved observing whether any significant drift in the centroids of certain background gamma-lines had occurred in the system over time. Spectra were recorded every 15 minutes on the maestro system. The acquired spectra were analysed using the Radware graphical package gf3 [Rad]. The original stability tests were done by collecting background spectra in which the 1460 keV and the 2614 keV background radiation peaks were analysed. These originate from the decay of the ^{40}K and ^{208}Tl, respectively. When collecting the background spectra, the amplifier was set to a shaping time of 2μs and a gain that yielded an energy range of about 2800 keV in 8192 channels. The results from the background spectra collected demonstrated a drift of about 2 channels over a weeklong period (1channel=0.36 keV, i.e. 0.7 keV for the two peaks analysed).

Tests were also carried out using an ^{152}Eu source and the shaping time was changed to 6μs, with a gain that gave an upper energy limit of 1550 keV in 8192 channels. Spectra were collected every 15 minutes and the 122 keV, 779 keV and 1408 keV peaks from this source were analysed. On analysing the spectra recorded from the ^{152}Eu

source (122 keV, 779 keV, 1408 keV) it was found that the drift is of the order of 1 - 2 channels (1channel = 0.2 keV, i.e. 0.2 - 0.4 keV for all 3 peaks) over a one-week period. The drift experienced over a 24 hour period was in the region of 0.1 - 0.2 channels (i.e. 0.02 - 0.04 keV for all three peaks) for this source. There was little drift experienced over the 15 minute data collecting period, and if any significant drift was noted (> 0.5 channels) these spectra were eliminated from further analysis. Based on these initial stability checks, we were able to select a set of NIM electronics/ NIM crate and cables for all future tests because we were confident about their stability over long periods of data collection.

2.3 Tinytag Data Loggers and the PT1000 signal

2.3.1 Tinytag Data Loggers

The ambient room temperature was monitored using Tinytag data loggers which were on loan from Sellafield [GDL]. Time was spent becoming familiar with the operation of these data loggers and tests were carried out to determine if there was any difference between their readings when placed side by side. It was found that the data loggers were reading very similar temperatures with a maximum variation between each temperature recorded of about 0.1 ^{o}C. The reading resolution accuracy of the Tinytag data logger is quoted as 0.01 ^{o}C or better [GDL].

2.3.2 PT1000 signals from Ge detectors

A PT1000 is an RTD (resistance temperature detector) sensor that is made from Platinum. A PT1000 has a resistance of 1000 ohms at 0 ^{o}C [Ome]. It was hoped at the beginning of the project that if the detectors had a PT1000 signal, it would be possible to record these via a Labview program [NI] so that a constant read out of the detector crystal temperature could be obtained. This would have allowed an investigation to be carried out to explore whether a change in the environmental temperature had any effect on the crystal temperature. The 3 detectors used did have such a signal but the method of read out for the 3 detectors was far too cumbersome to contemplate its use. It would have been necessary to remove the outer cover of the detector in order to access the electronics board where the PT1000 signal was located. This procedure would have to be carried out while the high voltage was turned off. As a result no measurements were made.

2.4 Multichannel Analyser (MCA) system

Initial tests were carried out using an Ortec 8k ADC and Maestro software system [Ortc]. In light of the fact that the main parameter being measured was the resolution, it was decided to purchase a 16k ADC (Ortec model no.927) [Ortd] in order to give better sensitivity to measurements of the FWHM. The ADC chosen could be powered from a standard NIM crate and used Universal Serial Bus (USB) interfaces to transmit data to a PC running the Maestro software.

2.5 Design of the Temperature Controlled Enclosure

The temperature range of interest for the detectors was $0 - 30^{o}$C and it was agreed to try and design an enclosure that would enable measurements to be made within this range. Discussions with manufacturers on the use of their detectors subsequently limited the operating range to $5^{o}\text{C} < \text{T} < 30^{o}\text{C}$. This limitation was due to the recommended operational temperature range for the compressor used in the Ortec X-cooler system.

The initial step was to design an enclosure that would in principle hold the environment at a stable temperature. It was also necessary to determine a method of controlling the temperature for this enclosure. It was decided that the best approach to take would be to design an insulated enclosure that would in theory hold the temperature inside this box stable. The Celotex insulation material (available from B & Q, a DIY store), which has a U-value of $0.1156\text{W/m}^2\text{K}$, was the material of choice. The U-value is a measurement of the ability of a material to transmit heat, the lower the U-value the greater the resistance to heat flow and therefore the better the insulator [Val]. Information also had to be obtained about the dimensions of the detectors to be received, in order to ensure that the box was going to be big enough to place these detectors inside and also to allow room for source placement in front of the detectors. The final dimensions and materials are as follows:
The frame of the enclosure consisted of a plywood exterior and was lined on all 6 panels with 100 mm thick Celotex insulation. The dimensions of the box were approximately 1000 mm wide, 1500 mm deep and 1800 mm in height.

Once these details were decided upon, the York technical staff built the enclosure to the required specifications (see Figure 2.1). The temperature in the enclosure was controlled using a matrix circulating system. This system consists of a pump that can be set at a specified temperature, which pumps heated / cooled water through

pipes into the enclosure. A small (slowly rotating) fan located at the back of the box disperses this heated / cooled air throughout the enclosure, thus ensuring uniform temperature in the box. The pumping system was located outside the enclosure in the large temperature-controlled clean room located at the University of York Nanocentre.

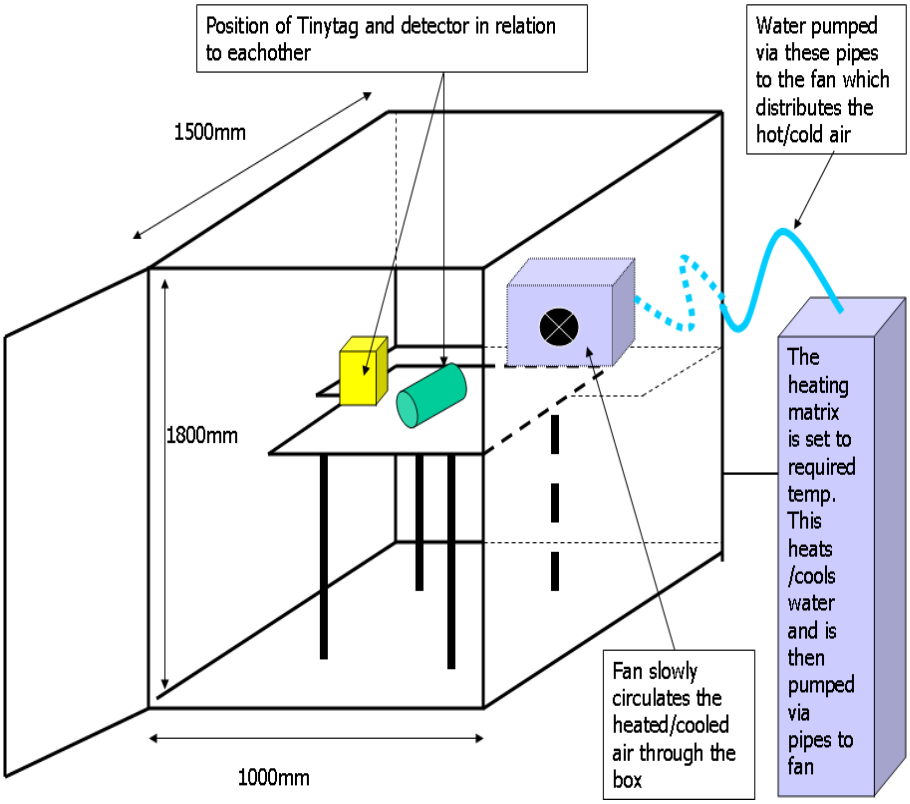

Figure 2.1: Schematic Layout and dimensions of the insulated box and cooling system used to control the temperature inside the box, displaying the close proximity of the Tinytag data logger and the detector, ensuring that the datalogger is recording the temperature of the region surrounding the detector.

2.6 Investigation of Temperature Stability

Tests were carried out using the Tinytag data loggers to investigate if the temperature in the newly constructed enclosure could be held constant without any detector in it and also to see over what range the temperature of the box could be controlled. These tests were carried out in the Physics Department. In addition, tests were also carried out to see whether external temperature fluctuations were mirrored inside the box. This latter test was performed in the Nanocentre. Initial tests carried out in

the Physics department were performed in order to establish if the temperature could be held constant in the empty box. The temperature in the enclosure was initially set to 2^oC and then 30^oC using the matrix system and the results were monitored using tiny tags (Figure 2.2a and 2.2b). After the temperature stabilised (2.5 hours) in the enclosure, the temperature was observed to remain constant at 5^oC and 29^oC respectively, with a variation of $< 0.5^oC$ between the upper and lower levels of the enclosure. Some of this temperature variation ($\sim 0.1^oC$) between the upper and lower levels in the enclosure may be attributable to the fact that the data loggers do not read the same temperature for the same environment(i.e. up to 0.1 ^{o}C variance as discussed earlier – see Figure 2.2c). The remaining difference ($<0.4^oC$) probably reflects the actual temperature variation within the box between the upper and lower levels.

In order to determine if external temperature fluctuations were mirrored inside the box in the Nanocentre, the matrix system was set to circulate at 25^oC, while the clean room in the Nanocentre was set at 20.5^oC. Two Tinytags were placed in the insulated box (upper and middle levels) and one placed in the clean room. The temperature variation was recorded. After about 4 hours the temperature of the clean room was increased to 23.5^oC (see Figure 2.2d). The result of this investigation demonstrates the fact that external temperature fluctuations are reflected in the temperature of the insulated box but that the effect is lessened by the fact that the box is well insulated (e.g. for a 3^oC change of temperature in the clean room, there is a corresponding change of $\sim 0.5^oC$ in the insulated box).

A problem identified during these tests was the fact that the temperature reached inside the box never matched the temperature that the matrix system was set to. It was also established that this difference is not constant for each temperature measured. At low temperatures the difference is $> 3^oC$ and at the higher temperatures it is $< 1^oC$. Adjustments to the water temperature will have to be made to achieve similar working temperatures for the different detectors. However, it is not essential that identical working temperatures are obtained for all detectors, just that the temperatures used cover a similar range overall.

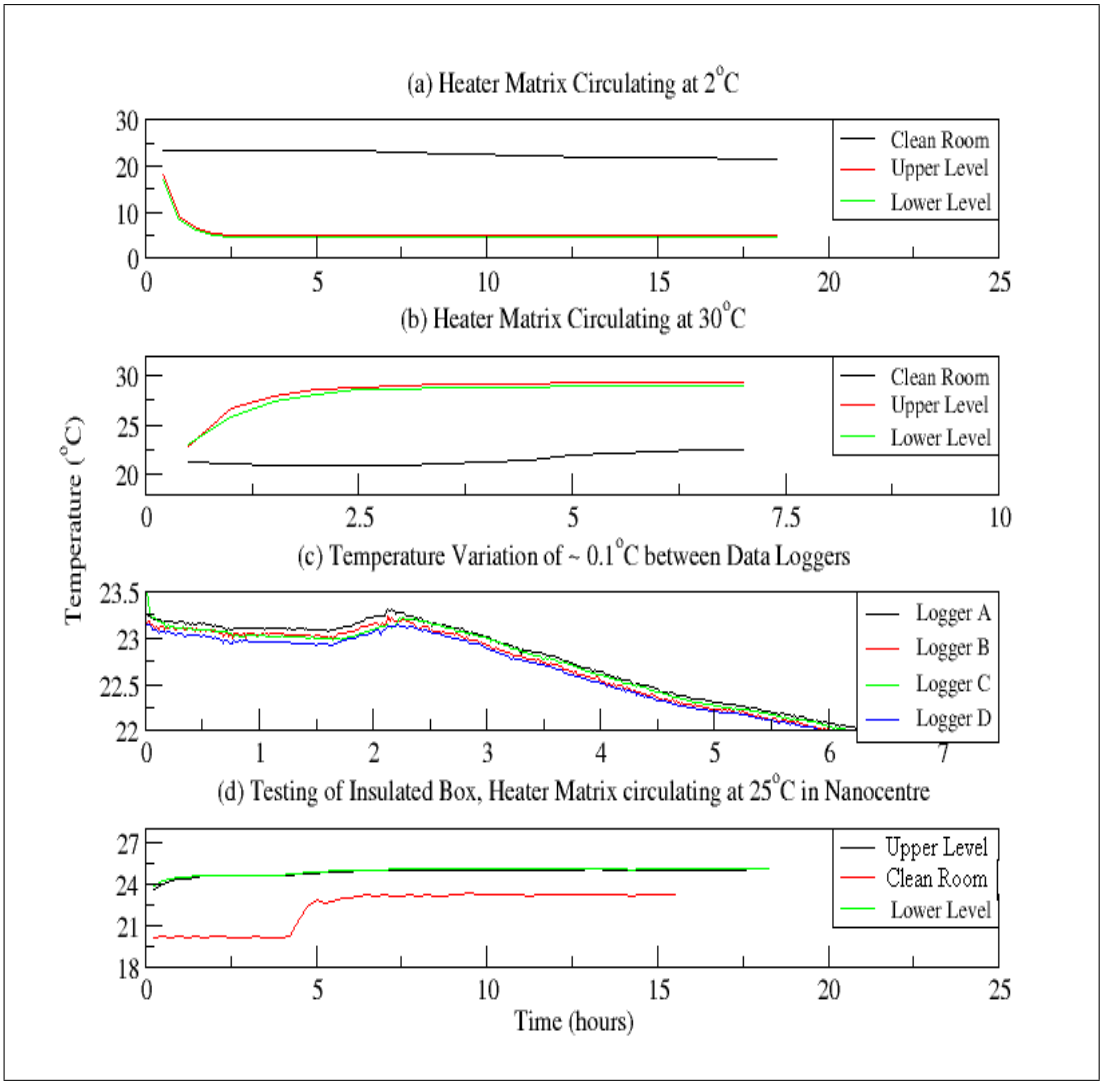

Figure 2.2: Plots (a) and (b) illustrates the stablity of the temperature recorded in the insulated box with the matrix set to 2^oC and 30^oC, respectively. Plot (c) demonstrates the temperature difference recorded between each of the 4 Tinytag Data loggers used at the beginning of the project. Plot (d) illustrates the fact that external fluctuations in temperature in the clean room are mirrored in the insulated box but to a much lesser degree due to the insulation.

2.7 The Final Experimental Parameters used in the Project

The following sections highlight the energy and temperature range of interest, count rate and shaping time and finally the data acquisition time used for all spectra taken.

2.7.1 Energy range of interest and Sources used

As indicated previously the prime energy range of interest to Sellafield was 50 - 150 keV. However it was agreed that the energy range selected for analysis would be from 60 keV up to 1408 keV. This was to be achieved using ^{241}Am and ^{152}Eu sources with activities of $\leq$ 370 kBq. In order to cover this wide range of energies for a final comparison, four gamma rays were chosen for analysis - 60 keV (from ^{241}Am), 122 keV, 779 keV and 1408 keV (from ^{152}Eu). A ^{60}Co source with an activity $\leq$ 370 kBq was used to carry out efficiency measurement for all three detectors. For the latter measurements the source was placed 25cm from the centre of the crystal.

2.7.2 Temperature range of interest

It was necessary to determine the temperature range that we firstly were interested in, and secondly, permitted to investigate by the manufacturers involved. It was concluded after consultation with the suppliers that the temperature range that we could work with was from $\sim 5^o$C up to $\sim 30^o$C for the Ortec detectors supplied and $\sim 10^o$C up to $\sim 30^o$C for the Canberra detector. As these were the minimum and maximum limits that we could work with it was decided to work from around 8^oC up to 28^oC for the Ortec detectors and from around 10^oC up to 28^oC for the Canberra detector.

2.7.3 Count Rate and Shaping time

The primary measurements were made under optimum counting conditions. For example, for the lower counting rates of around 1 kHz, a shaping time of 6μs was used on the amplifier. For higher counting rates of $\sim$ 20 kHz a shaping time of 2μs was used. A smaller shaping time is used at a higher count rate to reduce dead time. In each case the pole-zero on the spectroscopy amplifier was adjusted as appropriate before measurements were taken. Pile-up rejection was not used during the high count rate data collection periods of this experiment. The resolution obtained at the high count rates for all detectors may be improved by using pile-up rejection in the future.

2.7.4 Data acquisition time

It was necessary to determine a spectrum run time for the system in order to ensure that there was going to be enough counts in each peak to determine the resolution of the selected gamma ray lines. Initially, when using the 8k ADC, it was found that 15 minutes was a sufficient length of time to define a nice peak shape but once the 16k ADC was used this was found to be inadequate and this length of time had to be doubled. Thus for all measurements made in the Nanocentre individual run times of 30 minutes were used. The maestro software used could be set to save spectra after 30-minute intervals and then to automatically clear and restart the counting for subsequent periods, thus allowing the continuous collection of spectra over long periods.

Chapter 3

Experimental Setup in the Nano Centre

In June 2009, the experimental setup was moved to the Nanocentre in the University of York. This chapter describes the final experimental set-up in more detail. Section 3.1 presents the final setup of the temperature controlled enclosure and the heating/cooling matrix system. Section 3.2 displays the final electronic apparatus (NIM bin and NIM modules) used in all experimentation. Section 3.3 presents the Tinytag data loggers that were selected for the project, whilst section 3.4 presents the detectors used in this project, with sections 3.4.1, 3.4.2 and 3.4.3 displaying the specifications of the Ortec Xcooler Detector, the Ortec Liquid Nitrogen Dectector and the Canberra Cryo-cycle detector, respectively. The analysis package used in the project gf3 [Rad] is discussed in further detail in section 3.5. Finally, section 3.6 offers the final experimental procedure used for all detectors.

3.1 The temperature controlled enclosure

The temperature controlled enclosure, heating/cooling system and NIM bin were moved to the Nanocentre for the duration of the project (July - December 2009). The detectors were placed inside the insulated box with the electronics and computer located in the temperature-controlled room. This ensures that the electronics will be held at a constant temperature and thus limiting any effect their temperature fluctuation may have had on the measurements taken. The use of this location enabled the temperature of the clean room to be varied over a limited range, and hence allowed us to see if any effects on the resolution could be attributed to such changes.

The pump for the Ortec X-cooler detector was placed outside the temperature-controlled box and the detector placed on a wooden table in the middle of the insulated box. The Liquid Nitrogen cooled detector was also placed on this table. The pump for the Canberra cryocycle detector had to be placed inside the box and the heating effects of this pump had to be taken into account when selecting the temperature of the matrix system.

3.2 Electronic Apparatus

After completion of the initial tests described above, a final experimental setup was ready for action (June 2009). A block diagram of the electronics used in the project is provided in Figure 3.1. An Ortec 659 model bias supply was used with the detectors received from Ortec. Canberra supplied a 31060 high voltage power supply to use in conjunction with their detector. All detectors used an Ortec 572 spectroscopy amplifier, an Ortec 441 ratemeter and an Ortec 927 Aspec MCA. An oscilloscope was used when biasing up the detectors and adjusting the pole-zero. A PC loaded with maestro software was used to record the spectra and a pretested set of BNC and SHV cables were used for all detectors.

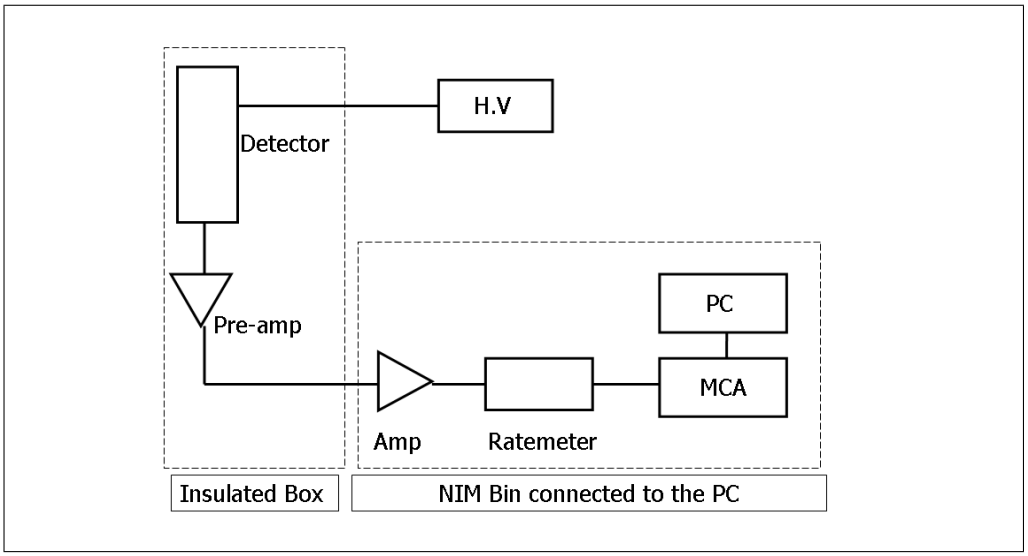

Figure 3.1: Block diagram of Electronics used in the Project

3.3 Tinytag Data Loggers

Two data loggers out of the four supplied by Sellafield were used in this project. The first was labelled as A (insulated box) and the second was labelled as B (clean room). Data logger A was placed inside the insulated box in close proximity to the detector being tested. This recorded the temperature fluctuations inside the insulated box. Data logger B was placed on a bench in the clean room in order to monitor the ambient room temperature. Both were set to record the temperature every five minutes for the duration of each run. These results were stored in the data loggers and subsequently downloaded to the PC to enable plots to be prepared which showed the variation of the temperature with time. The temperature recordings for all the data acquisition runs for the three detector are compiled in Appendix B.

3.4 Detectors used in the Project

A University of York $\sim$ 25% efficient n-type LN2 cooled detector was used to set up the system and to test out the electronics and temperature controlled box. In addition, three detectors were tested over the duration of this project. An electromechanically cooled germanium detector (x-cooler) and a Liquid Nitrogen cooled detector were received from Ortec and a Cyro-Cycle detector which was a hybrid electro mechanical/liquid nitrogen cooled detector was received from Canberra Eurysis.

3.4.1 Ortec Xcooler Detector

This detector is made from p-type Ge, with a diffused lithium contact on the outside surface and the thinner ion-implanted boron contact on the inside core [Orta]. This configuration is given the name GEM by Ortec. This is a GEM series HPGE coaxial detector system, with relative efficiency of 60%. The specifications of the detector are presented in Table 3.1.

Detector Model No	GEM60PST
Cryostat Configuration	Pop Top
Preamplifier Model	257P
Crystal Diameter	81.9 mm
Crystal Length	52.5 mm
End cap to crystal distance	4 mm
Window thickness	1.00 mm
Window Material	Aluminium
Inactive Ge - dead layer (outside surface)	700 μm
High Voltage Bias	Positive 3000 V

Table 3.1: Specifications of the Ortec Xcooler Detector.

3.4.2 Ortec Liquid Nitrogen cooled Detector

This detector is made from n-type Ge material with a diffused lithium contact on the inside core and the thinner ion-implanted boron contact on the outside surface [Ortb]. This configuration is given the name GMX by Ortec. This is a GMX series HPGe gamma-x HPGE Coaxial photon detector system, with a relative efficiency of 10%. The specifications of this detector are presented in Table 3.2.

Detector Model No	GMX-10190
Cryostat Configuration	SL-GMX
Dewer Model	30B
Preamplifier Model	257N
Crystal Diameter	47.4 mm
Crystal Length	51.0 mm
End cap to crystal distance	3 mm
Window thickness	0.3 mm
Window Material	Beryllium
Inactive Ge - dead layer (outside surface)	0.3 mm
High Voltage Bias	Negative 3000 V

Table 3.2: Specifications of the Ortec Liquid Nitrogen Cooled Detector.

3.4.3 Canberra Cryocycle Detector

This was a BE3825 model, n-type Broad Energy Ge (BEGE) detector with a relative efficiency of 23.3%. Further details on the configuration of this detector can be found in section 1.3.2. The specifications for this detector are presented in Table 3.3.

Detector Model No	BE3825
Cryostat Model	7500SL
Preamplifier Model	2002CSL
Active Diameter	70 mm
Active Area	3800 mm^2
Thickness	25 mm
Outer surface of End cap to crystal distance	5 mm
Window thickness	0.5 mm
Window material	Carbon Epoxy
High Voltage bias	Positive 4000 V

Table 3.3: Specifications of the Canberra Cryocycle Detector.

3.5 Graphical Analysis Package: gf3

The Radware analysis package gf3 [Rad] was used to analyse the spectra collected. This analysis package was available in the department and it was decided to use this instead of the Maestro fitting program because there were more options available on Radware to fit the spectra obtained from each detector. Three fitting functions were used in this analysis; FT1, AF1 and PK. Each function performs a least squares fit in order to fit the selected peak. The spectra obtained from the Ortec X-cooler detector were analysed using the function FT1. When using this fitting function, one has to define the limits of the spectrum region that you wish to fit. Using the cursor on the screen, one also selects an approximate position for the peak of interest. The spectra gathered from the Canberra cryocycle detector were analysed using the PK function. This function prompts you to select the peak of interest using the cursor provided. PK attempts to automatically determine the background below the selected peak and the

integration limits. The final set of spectra gathered from the Ortec Liquid Nitrogen cooled Detector were analysed using the function AF1. The AF function will iteratively search for a peak in the region of the spectrum that had been selected and then perform a least-squares fit on the located peaks. The FT1 function struggled to fit the spectra obtained from the Cryocycle detector and the Ortec liquid nitrogen detector. Both the FT1 function and the AF1 function struggled to fit the spectra obtained from the Canberra cryocycle detector so these were analysed using the PK function. In the ideal situation, it would have been preferable to have used the one fitting function for all the detectors tested in this project but practically, each individual detector had used one consistent method for extracting the required data. It should be noted that due to problems encountering while fitting the 779 keV and the 1408 keV peaks for both the low and high count rates of the Canberra cryocycle detector and the Ortec Liquid Nitrogen detector (continuous segmentation faults), it was necessary to use the AS function (Add spectrum) in gf3. This function allows one to add spectra together, in this case three 30 minute spectra were added together and this new peak was fitted. This will obviously have an effect on the resulting resolution of these peaks for these detectors, due to the gain shifts over the 90 minute period.

3.6 Final Experimental Procedure

The following procedure was carried out for each of the three detectors received. The detectors were cooled as specified by the manufacturers instructions. Once cold they were slowly biased up (increasing the voltage by a a few tens of volts each time) while the signal was observed on the oscilloscope. The signal is allowed to settle for a few seconds after each increase of voltage. If one observed a slight increase in noise of the signal every now and again, this is a sign of early breakdown and therefore one should allow extra time for the signal to settle. However if one observes a sudden, large increase in noise the voltage needs to be turned off as unfortunately breakdown has occurred [Leo94d]. Once biased up, the pole-zero on the 572 spectroscopy amplifier was adjusted as needed, in order to minimise the undershoot of the peak decaying back to the baseline as seen on the oscilloscope. The sources used were positioned along the axis of the detector to give a count rate on the ratemeter of 1000 counts/sec for the low count rate and of 20,000 counts/sec for the high count rate (pole-zero adjusted once more). The amplifier shaping time was set to 6μs for the low count rate and 2 μs for the high count rate. The gain was adjusted to yield an energy range of about 1500 keV

in 16k channels for all detectors. Spectra were only analysed for periods in which the temperature of the insulated box had stablised to a constant temperature ($\sim$ 2 hours).

With the sources in the required position, Tinytag A was placed in close proximity to the detector. Then the door of the enclosure was closed tightly and locked with a padlock. The latter being necessary to satisfy radiation safety rules for use of the sources in the clean room. Tinytag B was placed on a bench in the clean room. For each run, the heating/cooling matrix was set to a temperature between 5^oC and 30^oC, and the Tinytag data loggers were set to record a temperature reading every 5 minutes for the duration of the run. The Maestro software was programmed to record a spectrum every thirty minutes for a 24 or 48 hour period. This procedure was repeated for different temperatures within the required range for low count rates and high count rates for each detector being investigated. The detector received from Canberra was a combined electro cooler/LN2 dewar which enabled measurements to be made with the cooler switched on and the cooler switched off.

In order to investigate if variations of the clean-room temperature, in which the electronics used to process signals from the detectors were housed, had an effect on the resolution of selected gamma peaks, the temperature of the insulated box was held at 15^oC for the duration of these tests. The clean room temperature was then varied, increasing and decreasing the temperature by $\sim \pm 5^oC$. The Tinytag data loggers were set to record this variation in temperature.

Efficiency measurements were carried out using a ^{60}Co source that was placed 250 mm infront of the crystal face. The end-cap to crystal dimensions were obtained from the manufacturers before this measurement was made in order to take this into account when positioning the source infront of the detector. This spectrum was acquired for each detector. Table 3.4 presents the ^{60}Co source to detector distances used for the efficiency measurements for each detector.

Dimensions	Canberra Cryo-cycle Detector	Ortec Liquid Nitrogen Cooled Detector	Ortec X-cooler Detector
Endcap to crystal distance (mm)	4.5	3.0	4.0
Endcap thickness (mm)	0.5	0.5	1.0
Distance from Detector to ^{60}Co source (mm)	245	246.5	245.0

Table 3.4: Table of ^{60}Co source to detector distances used.

Photographs of the final experimental setup for each detector are provided in Appendix A.

Chapter 4

Results and Discussions

The following provides an overview of the analysed results for the three detectors used over the duration of this project. Typically 25 – 40 data points were used to determine the mean resolution and standard deviation for each detector at a given temperature, with each data point representing 30 minutes of counting time. Plots of the normalised resolution versus temperature (^{o}C) were made, for all detectors, at both low and high count rates. The normalised resolutions were obtained by dividing the value obtained for each resolution by the resolution measured at the lowest temperature for each detector. These results can be found in section 4.1.

Plots of the normalised resolution versus time were made for all data runs, to determine if any significant changes occurred in the resolution over time. However, in this thesis only an analysis of the 20 ^{o}C data run for each detector is shown in order to determine whether smaller selected samples of stable resolution may reduce the standard deviations and, in some cases, the resolution in the results presented in section 4.1. The results of this analysis are presented in section 4.2.

An investigation was also performed to assess if peak centroid drift had occurred over a seven day period (with each day representing an increase in temperature). One spectrum from each day of the data collection period was selected and a centroid position comparison was made over a week long period. These results are discussed in section 4.3. Small fluctuations in the clean room temperature were observed in the data downloaded from the Tinytag data loggers. There was concern over the possibility that these variations in temperature may have had an effect on the resolution measured. Analysis of the effect that these small fluctuations had on the recorded resolution was investigated. These results are discussed in section 4.4.

An investigation was carried out to determine if forced variations in the clean-room

temperature, in which the electronics used to process the signals from the detectors were housed, would have an effect on the resolution of the selected gamma peaks. These results are discussed in section 4.5. Since the electro-mechanical cooler of the hybrid electro-mechanical/Liquid nitrogen cooled detector from Canberra could be turned off for an extended period of time (24 hours), spectra were obtained (by switching off the cooler) to examine whether the cooler had an impact on the resolution of this detector. These results are presented in section 4.6. Finally in section 4.7, the absolute and relative efficiency of all three detectors is reported.

4.1 Analysis of the Resolution versus Temperature Plots

The results of the Resolution versus Temperature plots for all detectors at both low and high count rates are presented in sections 4.1.1 - 4.1.6. The plots are displayed in Figures 4.1 - 4.6, with the corresponding slopes (determined from a weighted least squares fit to the data) for each plot presented in tables following each figure (Tables 4.1 - 4.6).

4.1.1 Ortec Xcooler Detector – Low count rate plot.

Figure 4.1 presents the resolution versus temperature plot for the low count rate measurements for the four gamma peak energies 60, 122, 779 and 1408 keV. The mean resolution and corresponding errors were determined for four temperatures 9.4, 15.5, 19.8 and 24.4 ^{o}C. The resolution in each case was normalised relative to the lowest temperature i.e., the 9.4 ^{o}C resolution measurements. Table 4.1 presents the change in resolution as a function of temperature and also the percent change in resolution as determined by the best fit line points at the maximum and minimum temperatures recorded.

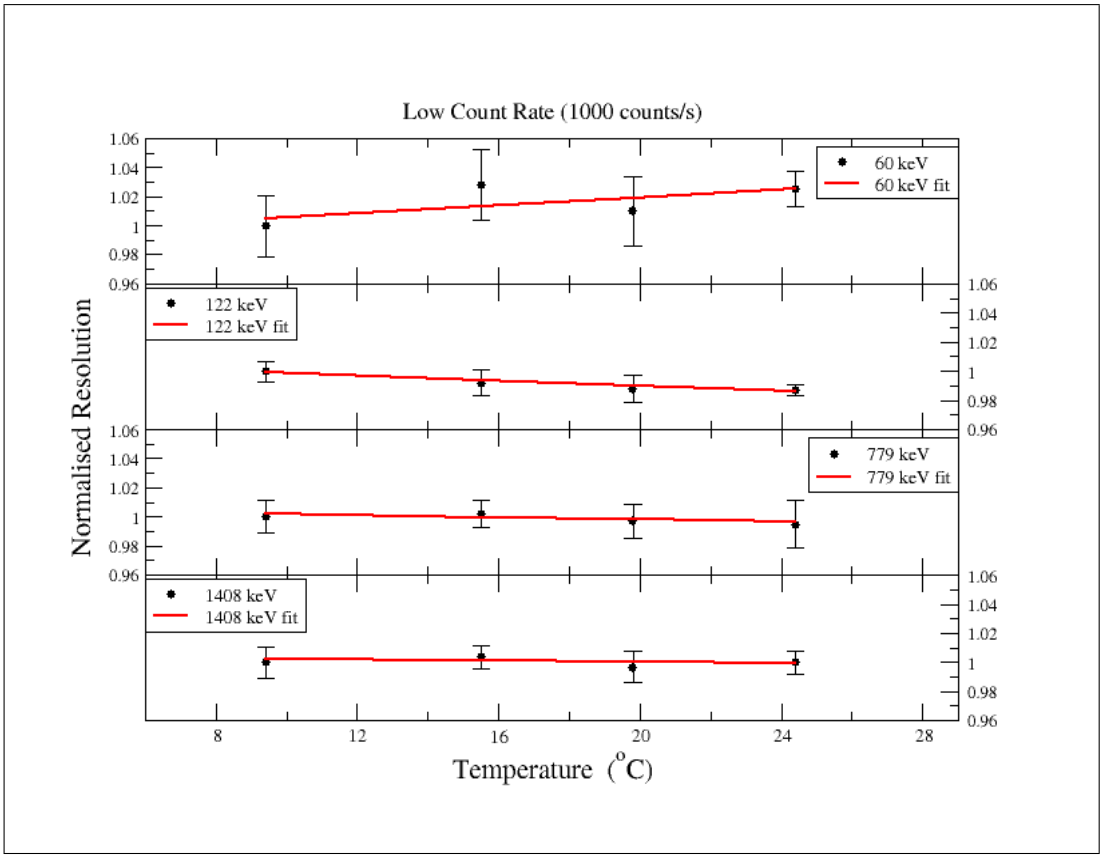

Figure 4.1: Plot of the normalised resolution versus temperature at a low count rate for the Ortec Xcooler detector for the 60 keV, 122 keV, 779 keV and the 1408 keV peaks.

Energy keV	Slope ($\Delta T = 15^o C$)	% Change in Resolution
60	0.0013 ± 0.0015	2.1 ± 2.4
122	-0.0008 ± 0.0005	-1.2 ± 0.7
779	-0.0003 ± 0.0008	-0.5 ± 1.3
1408	-0.0001 ± 0.0008	-0.3 ± 2.4

Table 4.1: Results showing change in resolution as a function of temperature. The table also shows the improvement or worsening of the resolution in percent terms at low count rates for the Ortec Xcooler Detector (see text for details).

On examination of Figure 4.1 and Table 4.1, it is apparent that there is little evidence for any significant change in resolution for any of the peaks analysed within errors.

4.1.2 Ortec Xcooler Detector – High count rate plot.

Figure 4.2 shows the resolution versus time plot for the high count rate measurements for this detector. The resolution of the four gamma peaks 60, 122, 779 and 1408 keV was extracted for five data runs at the following temperatures 6.8, 11.25, 15.7, 20.1 and 24.4 ^{o}C. The resolution has been normalised relative to the 6.8 ^{o}C resolution measurements. Table 4.2 presents the change in resolution as a function of temperature and also the percent change in resolution (as indicated in section 4.1.1) between the maximum and minimum temperatures recorded.

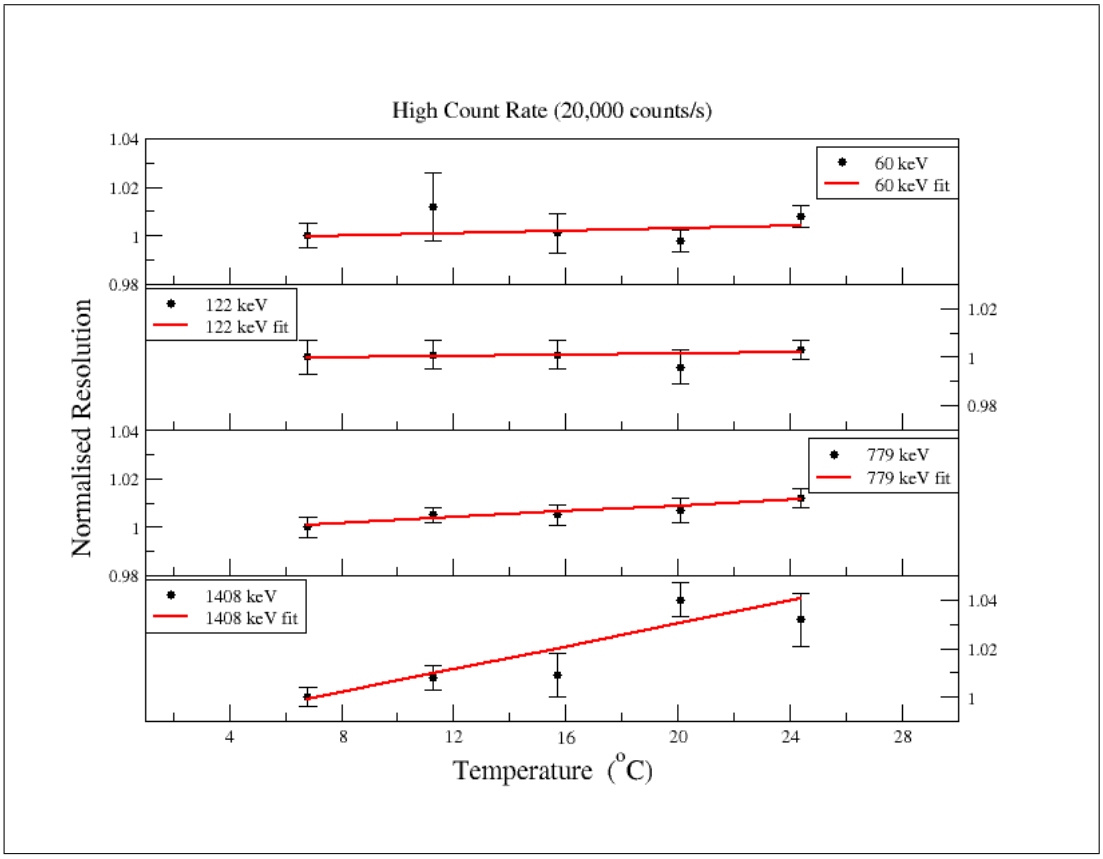

Figure 4.2: Plot of the normalised resolution versus temperature at high count rate for the Ortec Xcooler detector for the 60 keV, 122 keV, 779 keV and the 1408 keV peaks.

Energy keV	Slope (ΔT = 17.6^{o}C)	% Change in Resolution
60	0.0002 ± 0.0003	0.5 ± 0.7
122	0.0001 ± 0.0003	0.2 ± 0.6
779	0.0005 ± 0.0002	0.9 ± 0.4
1408	0.0023 ± 0.0004	4.1 ± 0.7

Table 4.2: Results showing change in resolution as a function of temperature. The table also shows the improvement or worsening of the resolution in percent terms at High Count Rates for the Ortec Xcooler Detector (see text for further details).

Examining the results given in Figure 4.2 and in Table 4.2, it is evident that there is no change in the resolution of the low energy gamma rays within errors. However, for the two higher energy transitions there would appear to be a small but statistically significant change in resolution of the order of 0.9(4)% and 4.1(7)%, respectively, for the 779 and 1408 keV transitions.

4.1.3 Canberra Cryocycle Detector – Low count rate plot.

Figure 4.3 presents the low count rate results for the Canberra Cryocycle detector. The resolution of the four gamma rays (60, 122, 779, 1408 keV) was determined for five different temperature settings in the insulated box (11, 16, 20, 24.75, 29.9 ^{o}C). The resolution was normalised relative to the 11 ^{o}C resolution measurement. Table 4.3 presents the change in resolution as a function of temperature and also the percent change in resolution (see section 4.1.1) between the maximum and minimum temperatures recorded.

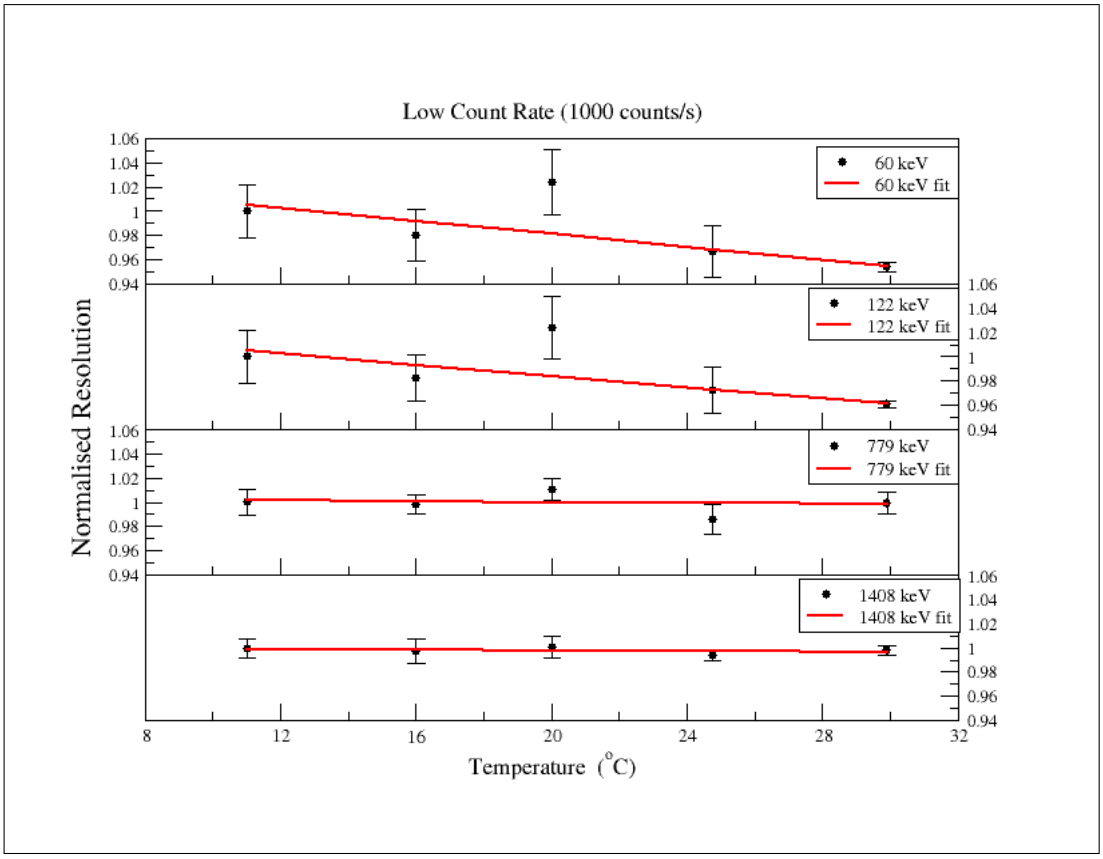

Figure 4.3: Plot of the normalised resolution versus temperature at a low count rate for the Canberra Cryocycle detector for the 60 keV, 122 keV, 779 keV and the 1408 keV peaks.

Energy keV	Slope ($\Delta T = 18.9^{o}C$)	% Change in Resolution
60	-0.0026 ± 0.0008	-5.3 ± 1.6
122	-0.0023 ± 0.0008	-4.5 ± 1.5
779	-0.0002 ± 0.0006	-0.4 ± 1.2
1408	-0.0001 ± 0.0004	-0.2 ± 0.8

Table 4.3: Results showing change in resolution as a function of temperature. The table also shows the improvement or worsening of the resolution in percent terms at Low Count Rates for the Canberra Cryocycle Detector (see text for details).

Table 4.3 reveals that the two lower energy transitions appear to show evidence for an improvement (i.e. decrease) in resolution (of the order of 5% between the maximum and minimum temperatures) as the temperature increases, whilst the two higher energy

transitions show little evidence of any change as a function of temperature. One noticeable feature is that the resolution observed for the 60 keV and the 122 keV gamma rays at 20 ^{o}C seems to be high relative to the other measurements. This feature is discussed further in section 4.2.1.

4.1.4 Canberra Cryocycle Detector – High count rate plot.

Figure 4.4 presents the resolution versus temperature results for the high count rate Canberra cryocycle Detector. Only three data sets were taken in this case due to time constraints before the detector had to be returned to the manufacturer. The resolution for the four gamma peaks (60, 122, 779 and 1408 keV) was determined for three temperature sets (12, 19.25 and 30.5 ^{o}C). The resolution in this case was normalised to the 12 ^{o}C resolution measurements. Table 4.4 presents the change in resolution as a function of temperature and also the percent change in resolution (see section 4.1.1) between the maximum and minimum temperatures recorded.

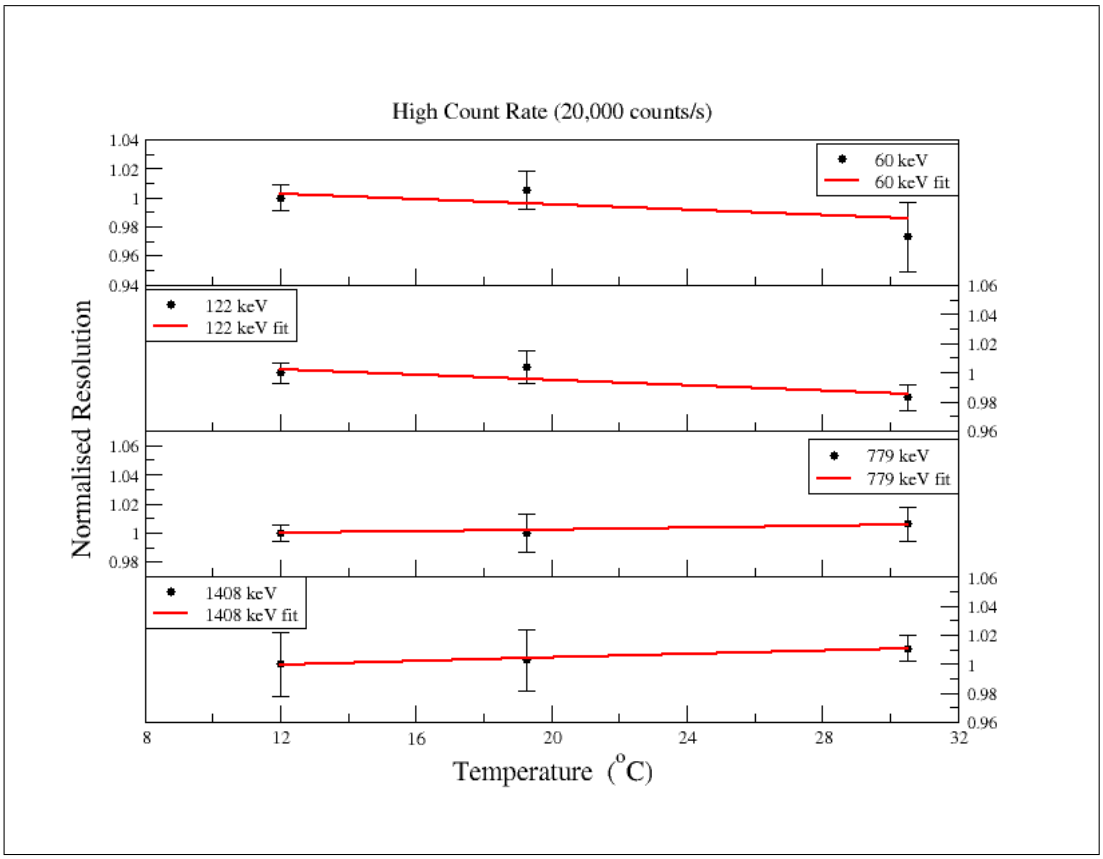

Figure 4.4: Plot of the normalised resolution versus temperature at a high count rate for the Canberra cryocycle detector for the 60 keV, 122 keV, 779 keV and the 1408 keV peaks.

Energy keV	Slope (ΔT = 18.5^{o}C)	% Change in Resolution
60	-0.0009 ± 0.0012	-1.7 ± 2.3
122	-0.0009 ± 0.0006	-1.7 ± 1.1
779	0.0003 ± 0.0007	0.6 ± 1.4
1408	0.0006 ± 0.0011	1.1 ± 2.0

Table 4.4: Results showing change in resolution as a function of temperature. The table also shows the improvement or worsening of the resolution in percent terms at high Count Rates for the Canberra Cryocycle Detector (see text for details).

The lack of data points clearly makes it difficult to comment with any degree of certainty on whether or not there is any significant effect. Within the error bars given in Table 4.4 it would appear that there is not a significant change in resolution as a function of temperature. However, given the results of the low count rate data for this detector one might argue that there is also weak evidence for a slight improvement in resolution as the temperature increases for the two low energy gamma rays (60, 122 keV). Further measurements would clearly be required to confirm this.

4.1.5 Ortec Liquid Nitrogen Detector – Low count rate plot.

Figure 4.5 presents the resolution versus time plot for the low count rate of this detector. The resolution has been determined for four gamma peaks (60, 122, 779 and 1408 keV), for six different temperature sets (6.5, 11, 15.2, 20, 24.5, 28.2 ^{o}C). The resolutions are normalised relative to the value obtained for the resolution of the 6.5 ^{o}C temperature set. Table 4.5 presents the change in resolution as a function of temperature and also the percent change in resolution (see section 4.1.1) between the maximum and minimum temperatures recorded.

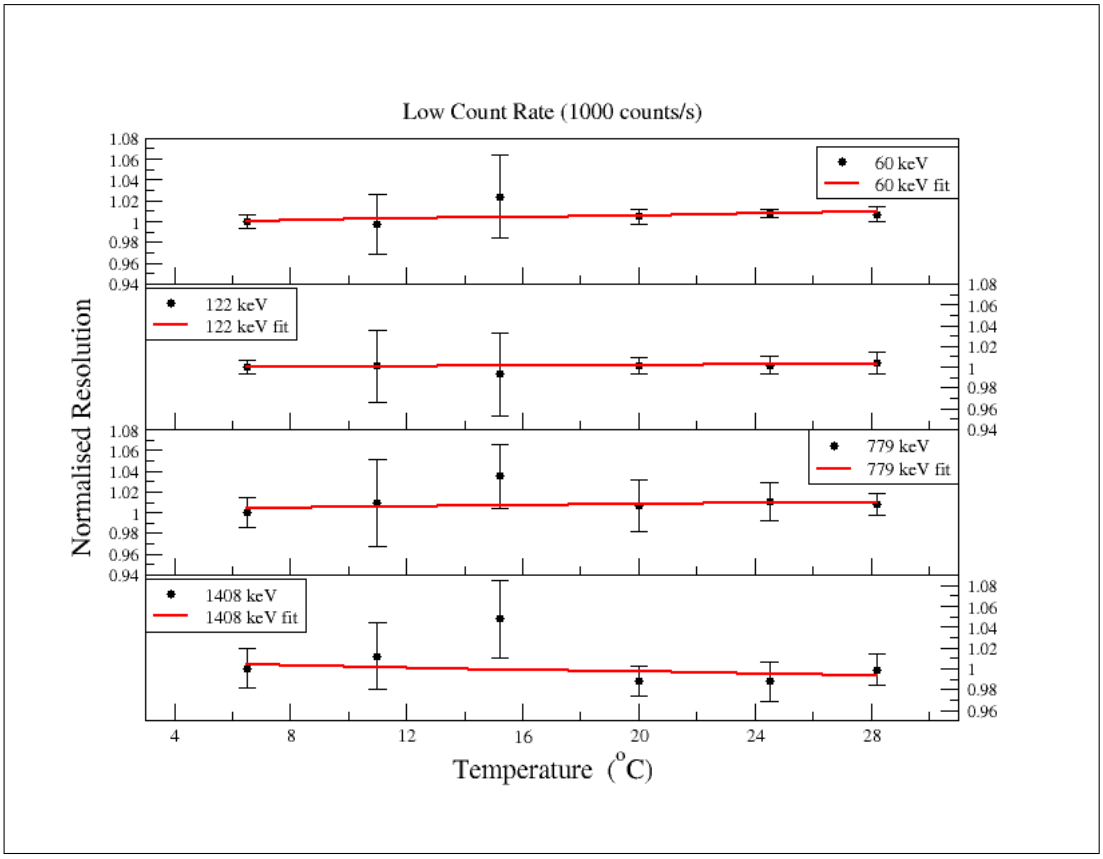

Figure 4.5: Plot of the normalised resolution versus temperature at a low count rate for the Ortec Liquid Nitrogen detector for the 60 keV, 122 keV, 779 keV and the 1408 keV peaks.

Energy keV	Slope ($\Delta T = 21.7^{o}C$)	% Change in Resolution
60	0.0003 ± 0.0004	0.8 ± 1.1
122	0.0001 ± 0.0004	0.3 ± 1.2
779	0.0001 ± 0.0007	0.7 ± 4.8
1408	-0.0004 ± 0.0010	-1.1 ± 2.8

Table 4.5: Results showing change in resolution as a function of temperature. The table also shows the improvement or worsening of the resolution in percent terms at Low Count Rates for the Ortec Liquid Nitrogen Detector (see text for details).

On examination of the results it is evident that there is no change in the resolution of the gamma rays as a function of ambient room temperature within errors.

4.1.6 Ortec Liquid Nitrogen Detector – High count rate plot.

Finally, Figure 4.6 presents the resolution versus temperature plot for the four gamma peaks (60, 122, 779 and 1408 keV) for four different temperature sets (6.5, 15.7, 6.5 and 25 ^{o}C). The resolution was normalised relative to the resolution value obtained for the 6.5 ^{o}C data acquisition run. On completion of the initial set of plots for resolution versus temperature, it was clear that there was a change of about 1 keV in the resolution measured for the 11 ^{o}C data acquisition run on this high count rate plot. From notes taken at the time this could be traced to the fact that the pole zero had not been correctly set for the 11 ^{o}C data. The pole zero was adjusted after this and remained fixed for the rest of the runs. Unfortunately the data for this particular temperature were not retaken due to time constraints and as a result this data set has been omitted from the final plot presented in Figure 4.6. Table 4.6 presents the change in resolution as a function of temperature and also the percent change in resolution (see section 4.1.1) between the maximum and minimum temperatures recorded.

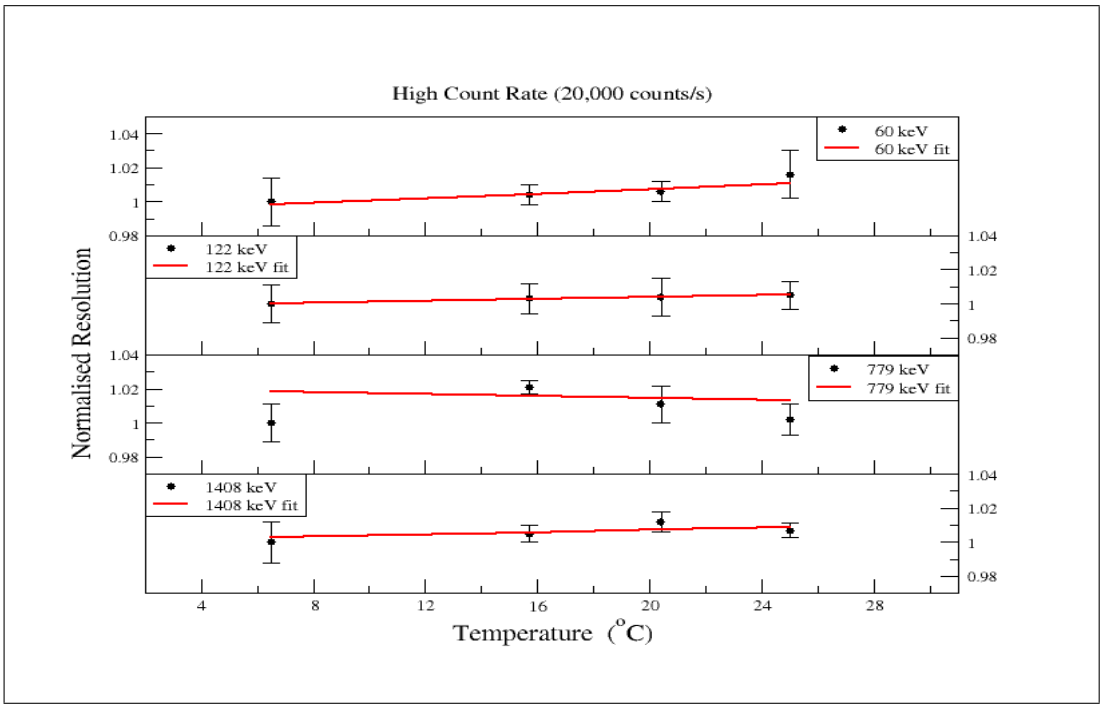

Figure 4.6: Plot of the normalised resolution versus temperature at a high count rate for the Ortec Liquid Nitrogen detector for the 60 keV, 122 keV, 779 keV and the 1408 keV peaks.

Energy keV	Slope (ΔT = 18.5^{o}C)	% Change in Resolution
60	0.0006 ± 0.0009	1.3 ± 1.9
122	0.0002 ± 0.0007	0.5 ± 1.7
779	-0.0002 ± 0.0007	-0.5 ± 1.7
1408	0.0002 ± 0.0005	0.6 ± 1.5

Table 4.6: Results showing change in resolution as a function of temperature. The table also shows the improvement or worsening of the resolution in percent terms at High Count Rates for the Ortec Liquid Nitrogen Detector (see text for details).

The information presented in Table 4.6 suggests once again that the resolution of the gamma peaks does not change within errors as a function of ambient room temperature.

4.2 Resolution versus Time plots

Graphs of resolution versus time for all data sets were plotted to observe the stability of the resolution recorded over time. Only a selection of these data plots are shown in the current section. Specifically, the data shown in Figures 4.7, 4.8 and 4.9 are for the T $\sim$ 20 ^{o}C measurements at low count rates for the Ortec Xcooler, the Ortec liquid nitrogen detector and the Canberra Eurysis Cryocycle detector, respectively. One of the reasons for choosing these data sets was that it was highlighted in Section 4.1.4 that there was an apparent problem with the larger than expected resolution being obtained at 20 ^{o}C for the 60 keV and the 122 keV gamma rays. In an attempt to explain why these fluctuations had occurred it was decided to select a smaller sample of data points for this detector run and calculate the mean resolution and standard deviation for this sample, in order to see if this varied significantly from the overall value obtained using all data points. The selection of the smaller sample of 10 data points was chosen to be in a region where the resolution appeared to be fairly stable for each detector. These results are compared with the original data (25-40 points) for the 20 ^{o}C run for the Canberra Cryocycle detector in Figure 4.9.

4.2.1 Analysis of the Resolution versus Time Plots

On examination of the plots for the Ortec Xcooler (Figure 4.7) and Liquid Nitrogen detector (Figure 4.8) it is evident that the resolution of all the gamma peaks are fairly stable over time. However, examining the Canberra Cryocycle plot (Figure 4.9) in further detail, it is apparent that for the low energy gamma peaks in particular, the resolution has a somewhat larger variation over time. This may be one factor contributing to the larger than expected resolution value obtained at 20 ^{o}C for these gamma peaks.

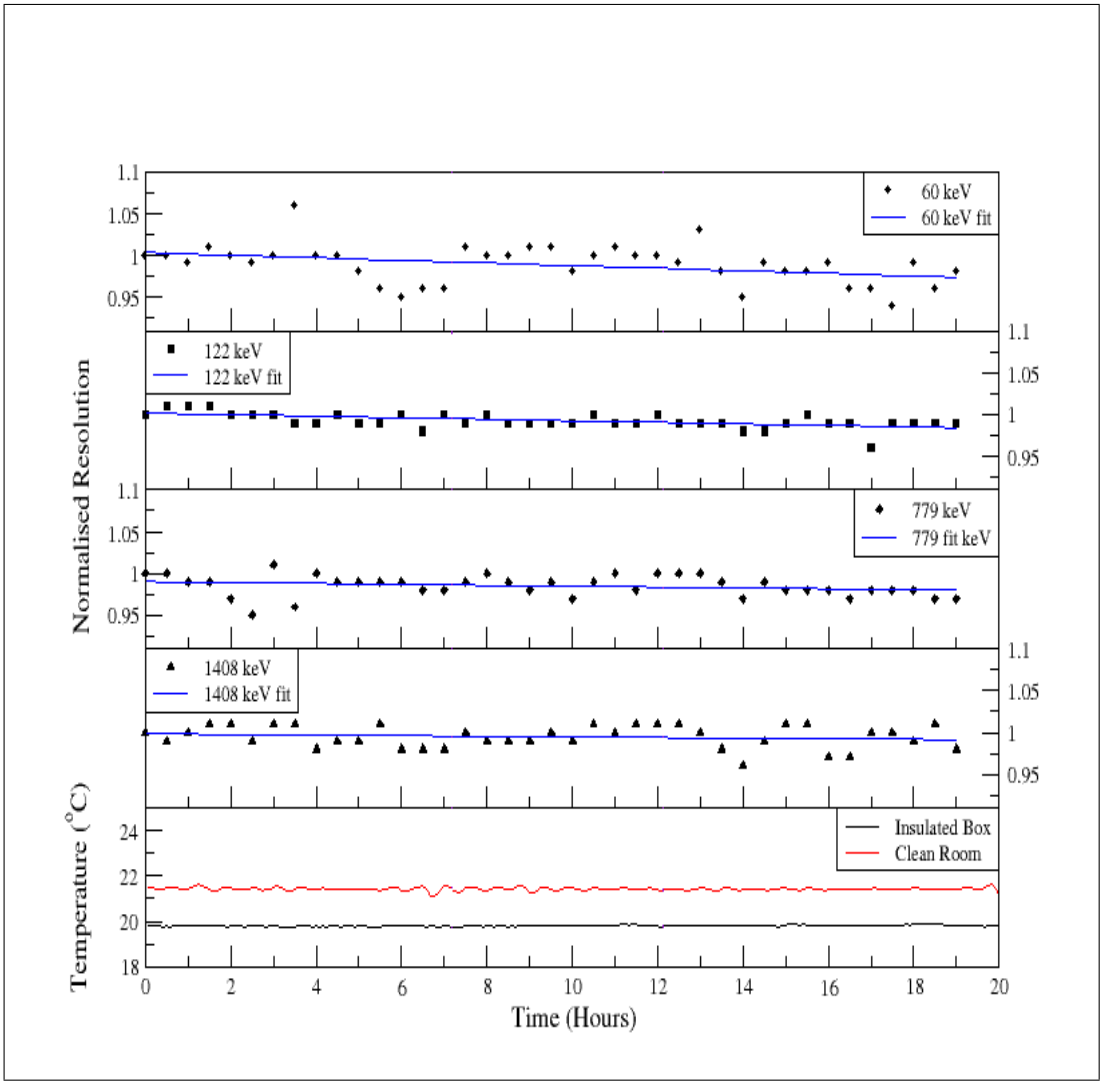

Figure 4.7: Resolution versus time plots for the 60, 122, 779 and the 1408 keV gamma peaks for the Ortec Xcooler detector. The temperature recording for this run is also presented. The oscillations present in the temperature plot are due to the temperature control system in the clean room. The error bars are typically in the order of 6% on the resolution versus time measurements.

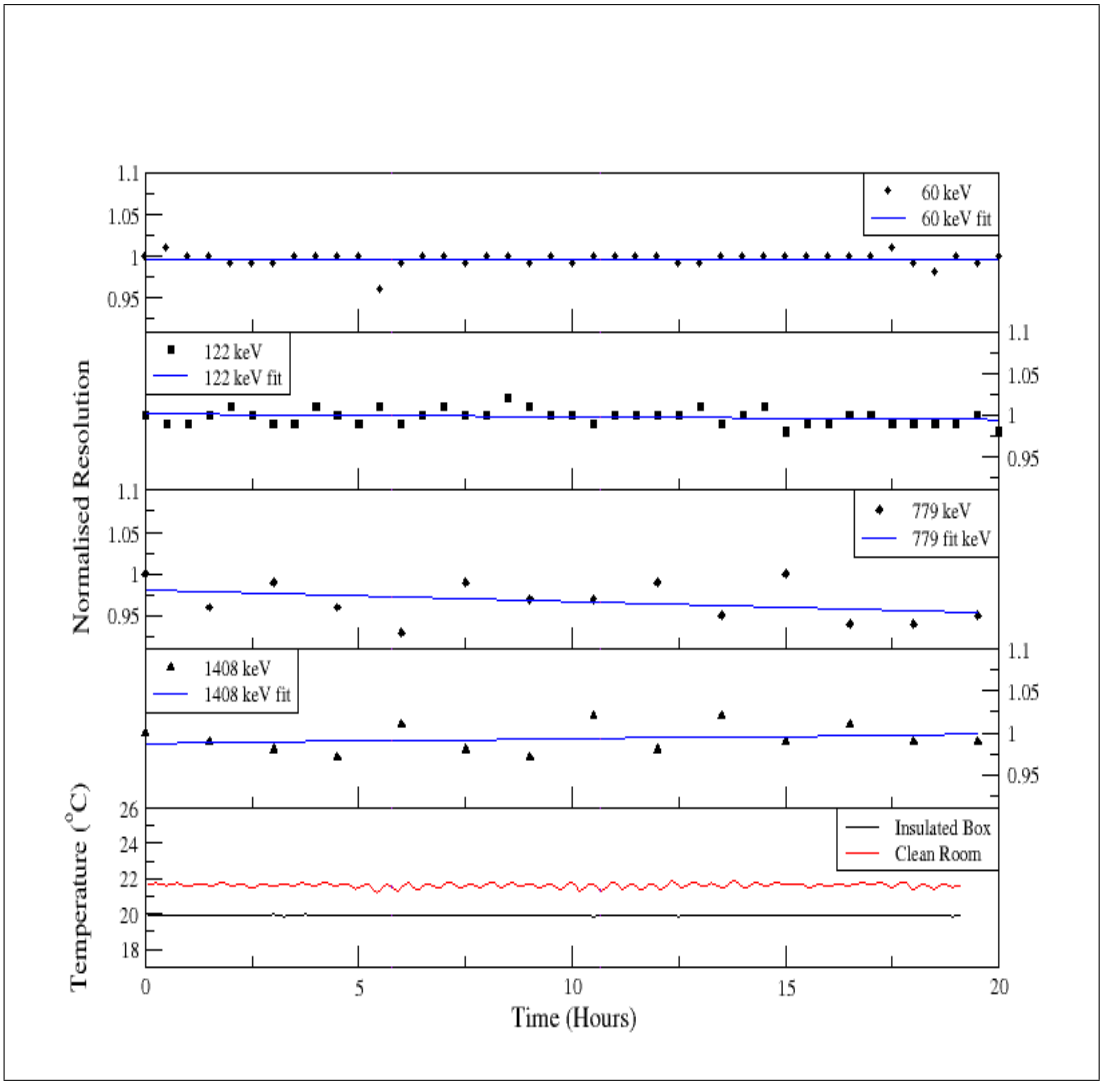

Figure 4.8: Resolution versus time plots for the 60, 122, 779 and the 1408 keV gamma peaks for the Ortec Liquid Nitrogen detector. The temperature recording for this run is also presented. The oscillations present in the temperature plot are due to the temperature control system in the clean room. The error bars are typically in the order of 5% on the resolution versus time measurements.

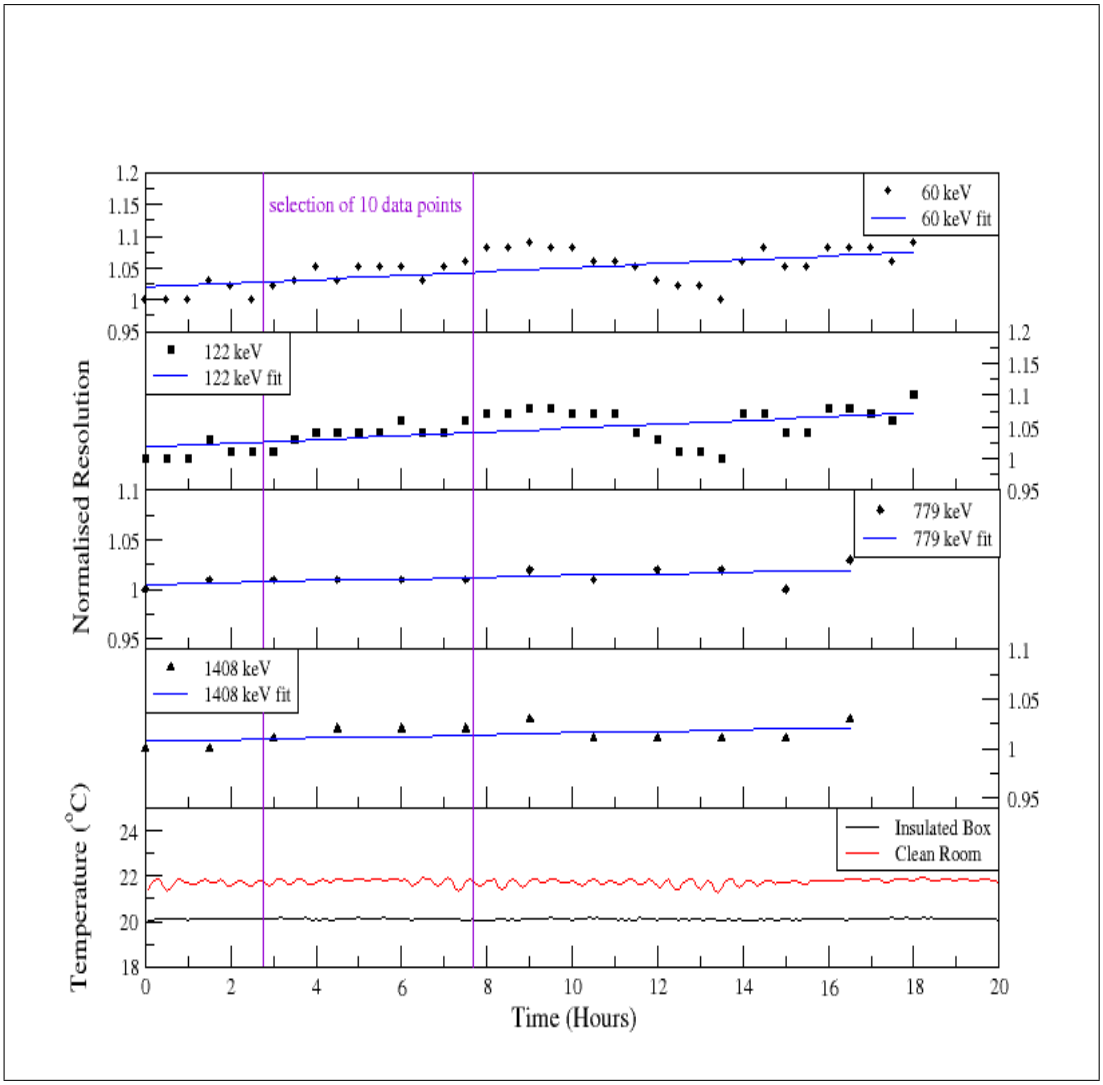

Figure 4.9: Resolution versus time plots for the 60, 122, 779 and the 1408 keV gamma peaks for the Canberra Cryocycle detector. The temperature recording for this run is also presented. The oscillations present in the temperature plot are due to the temperature control system in the clean room. The error bars are typically in the order of 6% on the resolution versus time measurements.

Figure 4.9 illustrates the selection of 10 data points for the 60 and 122 keV peaks, with a selection of 4 data points for the 779 and 1408 keV (due to the addition of the spectra needed for these peaks - see section 3.5 for further details). This selection was made based on the most stable region of resolution for the 60 and 122 keV peaks. The resolution was determined for the smaller sample and normalised relative to the resolution obtained for the mean of the original 36 data points. The normalised sets of resolution data and the percent change between these data sets are presented in Table 4.7. This percent change in resolution is defined by the difference between the

normalised mean of the original set of data points and the normalised mean of the new set of data points, divided by the original set of data points.

Energy keV	Mean Resolution of 36 data points (normalised)	Mean Resolution of 10 data points (normalised)	% Change in Resolution
60	1.00 ± 0.03	0.99 ± 0.03	1.2 ± 3.8
122	1.00 ± 0.03	0.99 ± 0.03	0.9 ± 3.5
779	1.00 ± 0.01	0.99 ± 0.01	0.6 ± 1.4
1408	1.00 ± 0.01	0.99 ± 0.01	0.3 ± 1.5

Table 4.7: The mean resolution of 10 data points is normalised relative to the mean resolution of the original 36 data points for the 60, 122, 779 and 1408 keV gamma peaks for the Cryocycle detector. The percent change between these two data sets is also presented (see text for details).

After careful examination of the results presented in Table 4.7, the change in resolution is not statistically significant within errors.

4.3 Drift of Peak Centroids

In an attempt to identify other potential sources that may contribute to the small variations in the results, the effect of centroid drift over time was investigated for different data acquisition runs and for different temperatures. One spectrum from each day of the data collection period was selected (the first spectrum observed for stable temperature) and a centroid position comparison was made over a seven day period. The results indicated that centroid drift was more noticeable for higher energy gamma peaks at both low and high count rates. This effect was most evident in the Ortec Xcooler detector in which an increase of 20 and 26 channels was observed for the 1408 keV gamma peak at high and low count rates, respectively, over a week long period. The remaining two detectors showed changes of <10 channels during the whole data taking process for all gamma peak energies, at both low and high count rates. This should be compared with the stability tests mentioned in section 2.2 which indicate that a drift of up to 4 or 5 channels might be anticipated (with the current ADC) in this period.

The plots of percent change in centroid position versus temperature (^{o}C) for low and high count rate measurements for the Ortec X-cooler detector is shown in Figure 4.10. The centroid position is relative to the position at the lowest temperature recorded for the low and high count rate data. Hence by definition there is 0% change at the lowest temperature recorded. Figure 4.11 shows partial spectra for the 1408 keV gamma ray and the amount of drift experienced over a four day period (each peak represents one spectrum for each day investigated during the low count rate measurements). Table 4.8 provides a colour legend for Figure 4.11. Each individual spectrum displayed in Figure 4.11 is one thirty minute run from the dates specified in Table 4.8. Figure 4.12 presents the temperature recordings for the 4 days of the data acquisition runs and the point in time that the spectra were selected in each case is marked on this plot.

Whilst this centroid drift is quite clearly observed for the 1408 keV peak, it has had minimal effect on the resolution measurements suggesting that the changes were occurring on a longer time scale relative to the sampling period. In terms of percent change of centroid position the three (122, 779 and 1408 keV) and gamma peaks plotted exhibit similar trends.

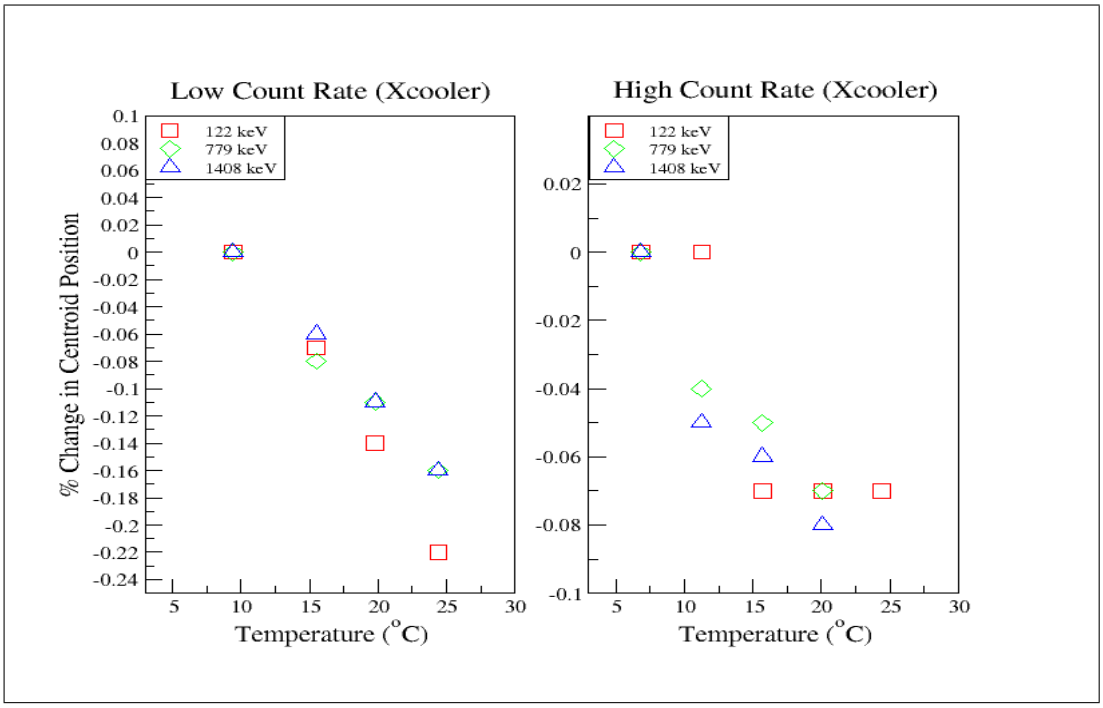

Figure 4.10: Examination of the percent change in Centroid position (relative to the lowest temperature measured) as a function of temperature for the Ortec X-cooler for the low and high count rates for the 4 gamma peaks, 60, 122, 779 and 1408 keV. The error bars on the centroid position are typically of the order of 5%.

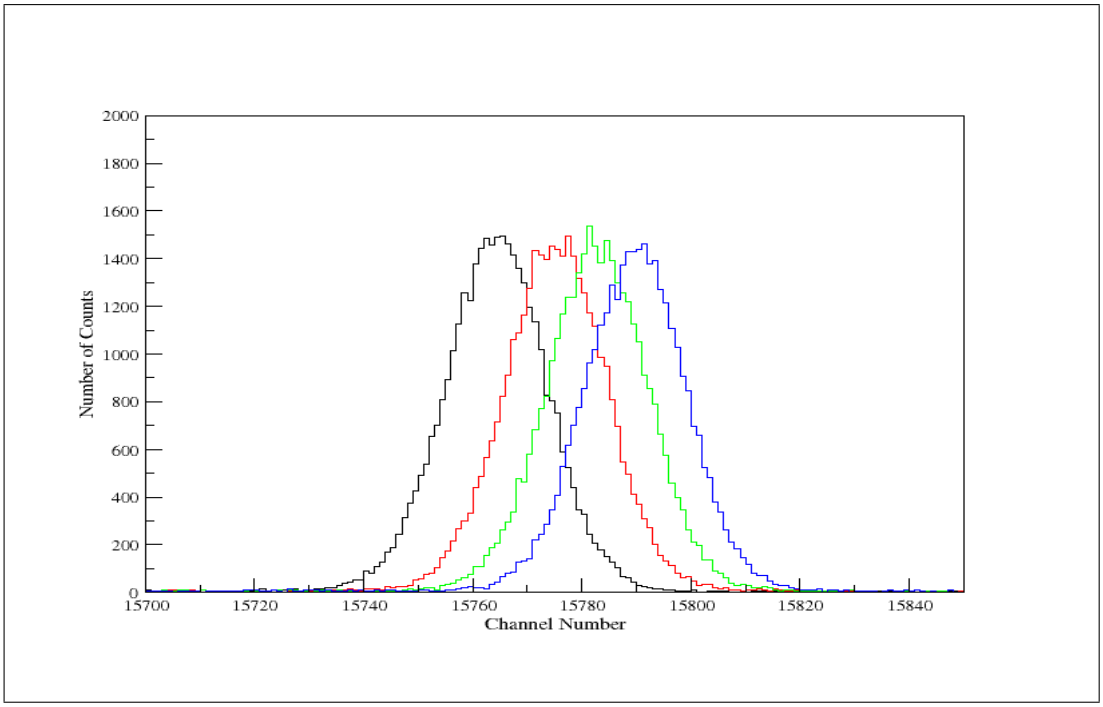

Figure 4.11: This displays the drift experienced by the 1408 keV gamma ray over a four day period for the Ortec X-cooler Detector at low count rates.

Name of Spectrum run	Colour	Date of Run	Centroid Position	Insulated Box Temperature ^{o}C	Clean Room Temperature ^{o}C
9xcooler	Black	27/08/09	15765	9.45 ± 0.01	21.51 ± 0.01
10xcooler	Red	28/08/09	15776	15.56 ± 0.01	21.41 ± 0.01
11xcooler	Green	01/09/09	15783	19.82 ± 0.01	21.51 ± 0.01
12xcooler	Blue	02/09/09	15791	24.41 ± 0.01	21.49 ± 0.01

Table 4.8: Provides the colour legend for Figure 4.11. This data represents the data acquisition runs at a low count rate for the Xcooler detector. This also presents the dates for each of the data acquisition runs in question, the centroid position recorded for each of these dates and the average temperature recorded in the insulated box and clean room.

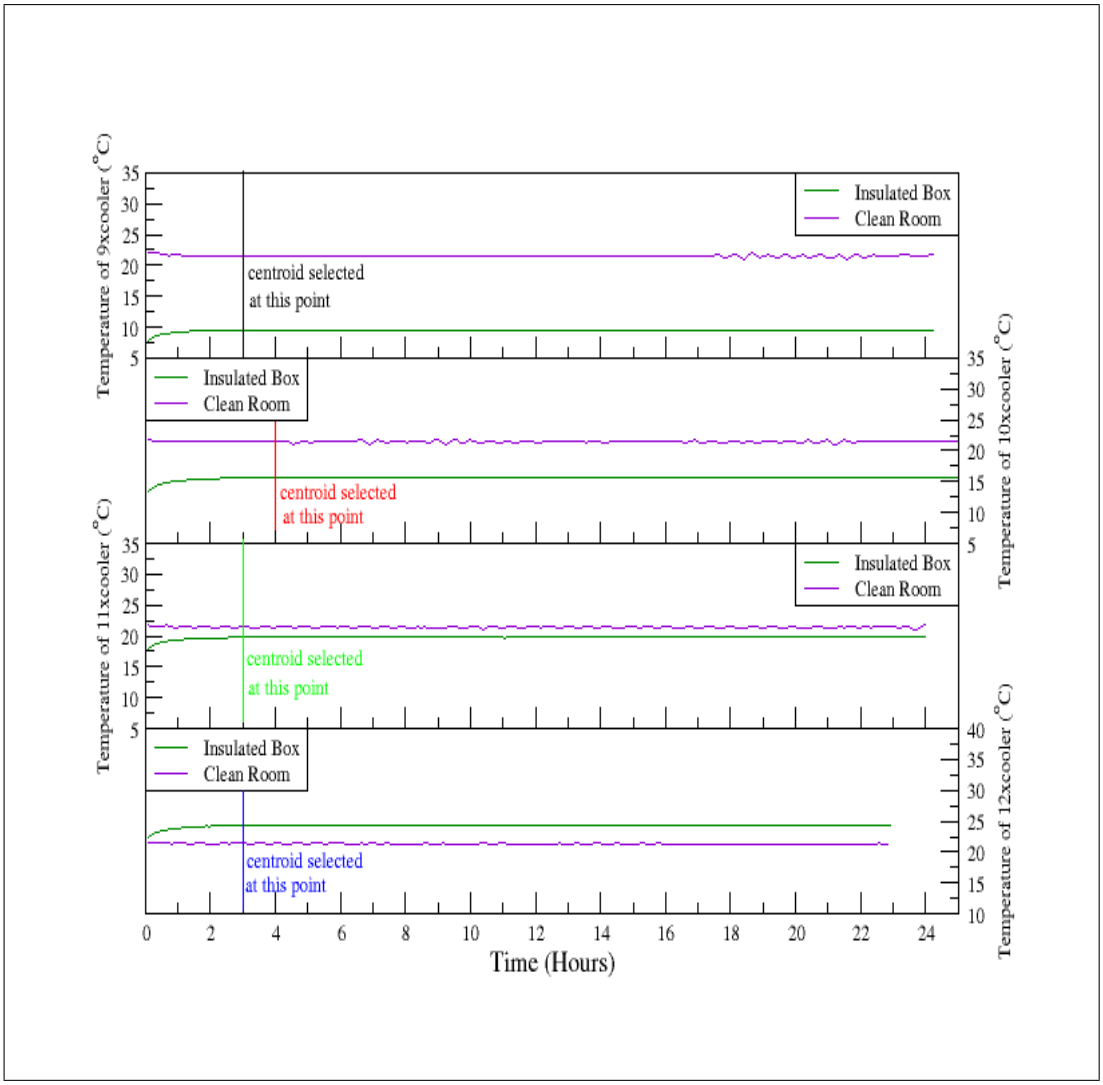

Figure 4.12: The temperature recordings of the Clean Room and Insulated Box for the 9xcooler (top), 10xcooler, 11xcooler and 12xcooler (bottom) runs. The vertical line in each plot represents the data point selected for analysis in each case. The position of these points were chosen as the first spectrum observed for stable temperature in each case. The oscillations present in these plots are due to the temperature control system in the clean room.

4.4 Fluctuations in the Temperature of the Clean Room

Small fluctuations in the clean room temperature were observed in the data downloaded from the Tinytag data loggers. There was concern over the possibility that this may have had an effect on the resolution measured during this variation in temperature. Two examples of this temperature fluctuation were examined in further detail, The Ortec X-cooler detector is investigated in section 4.4.1 with the Canberra Cryo-cycle detector discussed in section 4.4.2.

4.4.1 The Ortec X-cooler Detector

Figure 4.13 presents a plot of the resolution recorded during periods of stable and unstable temperature regions. The stable region is indicated by the blue markers, with the unstable region indicated by the orange markers.

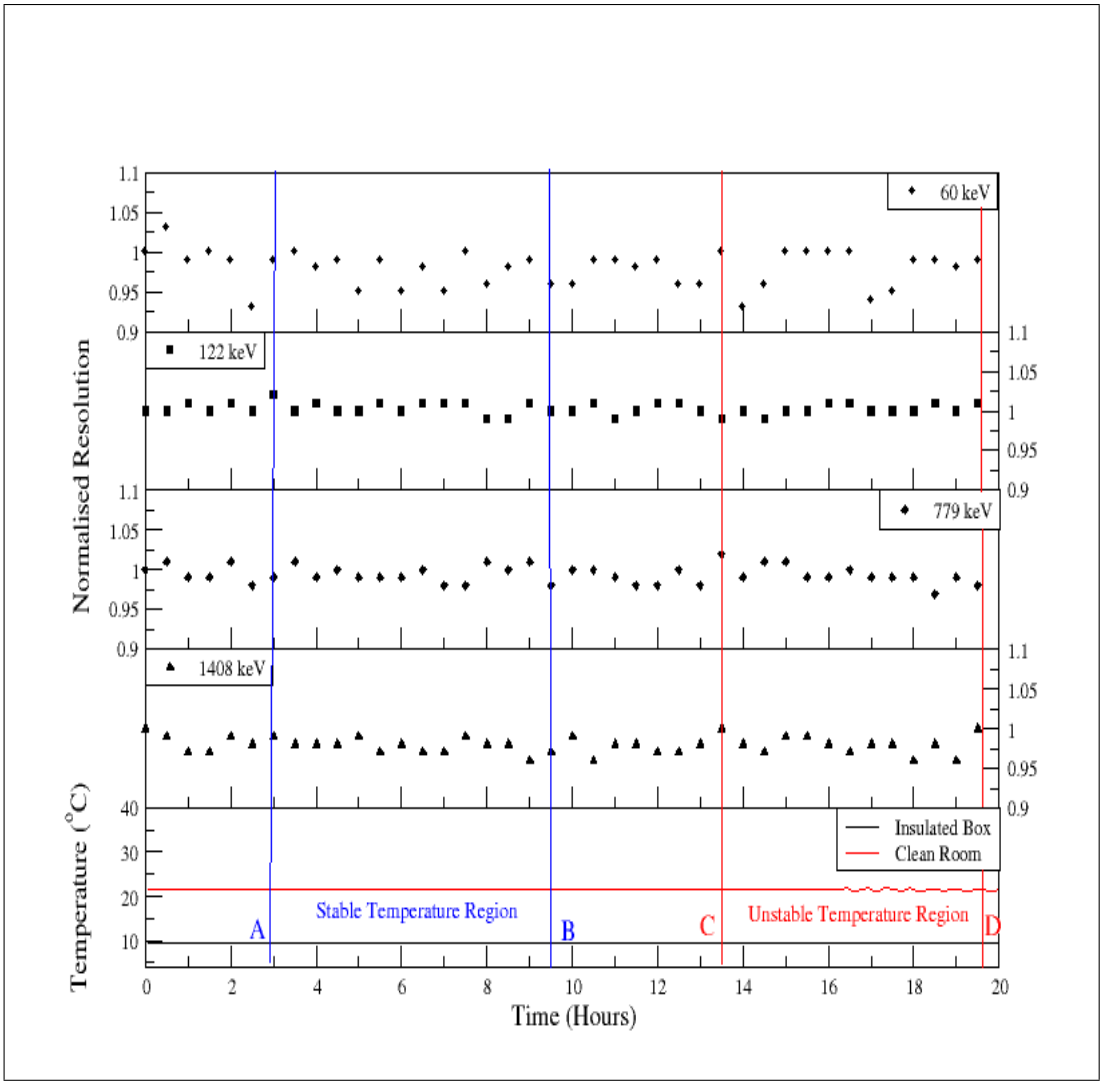

Figure 4.13: Plot of the normalised resolution versus time plots and the temperature recorded for the Insulated Box and Clean Room over the duration of the 9xcooler run of the Ortec Xcooler detector with regions of stable (blue) and unstable (orange) temperatures selected for further investigation. The oscillations present in the temperature plot are due to the temperature control system in the clean room. The error bars are typically in the order of 4% on the resolution versus time measurements.

Small temperature fluctuations (e.g. the orange region C-D) are evident in the temperature of the clean room in Figure 4.13. Regions of stable (blue A-B) and unstable (orange C-D) temperature have been selected and the mean resolution and standard

deviation for these regions were determined and a comparison made. The resolution of the unstable temperature region was normalised relative to the resolution obtained for the stable temperature region in all cases. By definition this means that the normalised resolution in the stable temperature region is one with an error that can be determined from the unnormalised resolution value. The results of the normalised resolution are presented in Table 4.9. The percent change between these two normalised data sets are also displayed in this table. This is defined by the difference between the normalised resolution obtained for the stable and unstable temperature readings divided by the normalised resolution for the stable temperature readings.

9xcooler run	Normalised Resolution for stable temp (A-B)	Normalised Resolution for unstable temp (C-D)	% Change in Resolution
60	1.00 ± 0.02	1.01 ± 0.03	-0.5 ± 4.0
122	1.00 ± 0.01	1.00 ± 0.01	-0.1 ± 1.1
779	1.00 ± 0.01	0.99 ± 0.02	0.1 ± 1.7
1408	1.00 ± 0.01	1.00 ± 0.01	0.0 ± 1.6

Table 4.9: The results of the resolution for unstable temperature region (C-D) is normalised relative to the resolution obtained for the stable temperature region (A-B) for the 60, 122, 779 and 1408 keV gamma peaks for the Ortec Xcooler detector. The percent change between these two data sets are also presented (see text for details).

It is evident from the results in Table 4.9, that these temperature fluctuations ($\pm 0.5^{o}$C) had little effect within errors on the resulting resolutions. Therefore it can be assumed that data from regions of both stable and unstable temperature can be used to determine the mean resolution and standard deviation in all cases. One can also confirm that within these operating parameters one can say that the detector system is stable.

4.4.2 The Canberra Cryocycle Detector

A similar method of analysis to that discussed above was used to determine if the resolution measured was influenced by the temperature fluctuations observed in the clean room during the 7combo run for the Cryocycle detector. The regions of interest are displayed in Figure 4.14. It should be noted that there are fewer points selected for the 779 and 1408 keV plot because of the addition of these spectra due to problems with fitting single 30 minute peaks (see section 3.5 for further details). The resolution

of the unstable temperature region was normalised relative to the resolution obtained for the stable temperature region in all cases. The results of the normalised resolution are presented in Table 4.10. The percent change between these two data sets are also displayed in this table (see section 4.4.1.).

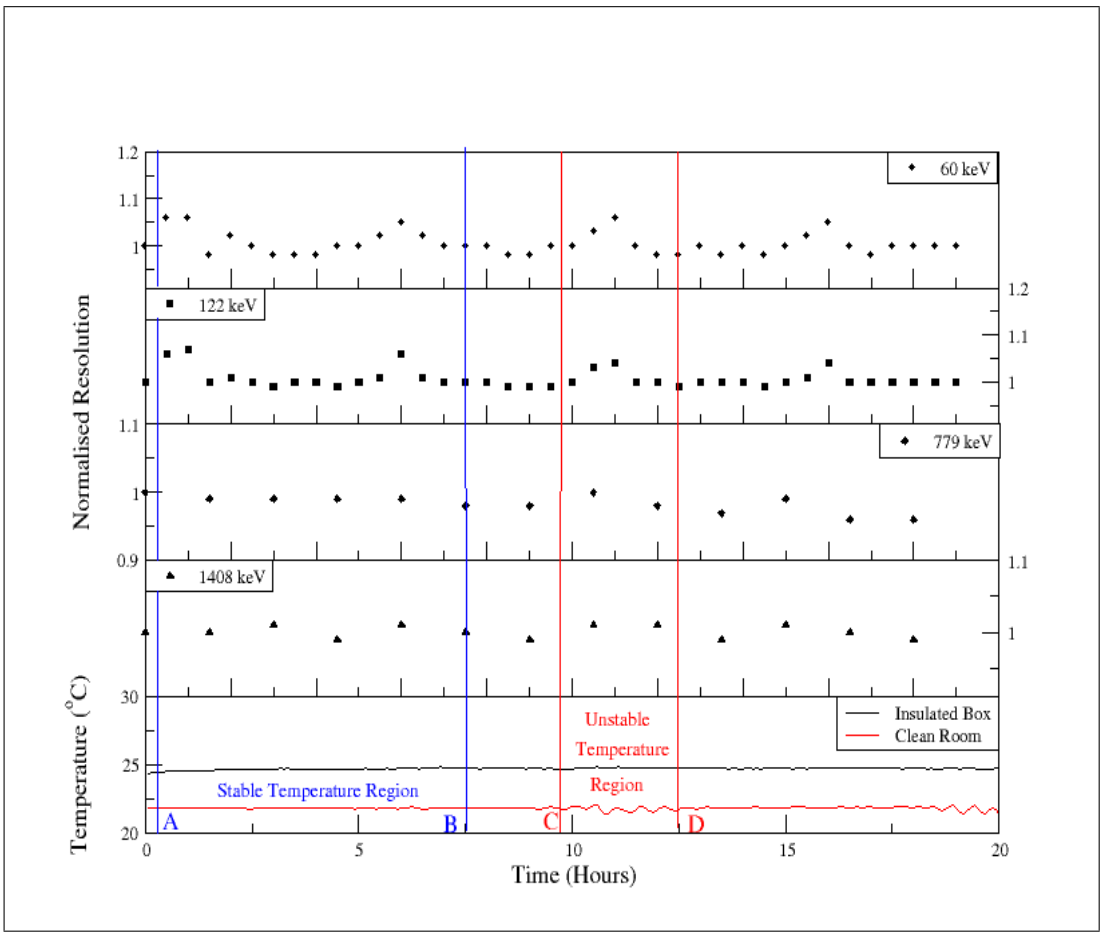

Figure 4.14: Plot of the normalised resolution versus time plots and the temperature recorded for the Insulated Box and Clean Room over the duration of the 7combo run of the Canberra Cryocycle detector with regions of stable (blue) and unstable (orange) temperatures selected for further investigation. The oscillations present in the temperature plot are due to the temperature control system in the clean room. The error bars are typically in the order of 5% on the resolution versus time measurements.

7combo run	Normalised Resolution for stable temp (A-B)	Normalised Resolution for unstable temp (C-D)	% Change in Resolution
60	1.000 ± 0.033	0.990 ± 0.037	1.0 ± 4.9
122	1.000 ± 0.029	0.992 ± 0.034	0.8 ± 4.4
779	1.000 ± 0.007	0.978 ± 0.018	2.2 ± 1.9
1408	1.000 ± 0.003	1.000 ± 0.095	0.0 ± 9.5

Table 4.10: The results of the resolution for unstable temperature region (C-D) is normalised relative to the resolution obtained for the stable temperature region (A-B) for the 60, 122, 779 and 1408 keV gamma peaks for the Canberra Cryocycle detector. The percent change between these two data sets are also presented (see text for details).

These results show that the temperature fluctuations experienced in the clean room ($\pm 0.5\ ^{o}$C) has little effect within errors on the resolution measured over the duration of these fluctuations for the Canberra cryo-cycle detector. Therefore it can be assumed that all data can be used for regions of stable and unstable temperature regions when determining the mean resolution and standard deviation.

4.5 Temperature variation of electronics

Results from the temperature variation of the electronics are now discussed. The temperature of the box was held at 15 ^{o}C for the duration of this test. The clean room temperature was then varied and the resolution and standard deviation for each detector measured for the 60, 122, 779 and 1408 keV gamma rays. The Ortec X-cooler detector, the Cryo-cycle detector, and the Liquid Nitrogen detector are discussed in section 4.5.1, section 4.5.2 and section 4.5.3, respectively.

4.5.1 The Ortec X-cooler Detector

Figure 4.15 shows the temperature of the clean room and the insulated box as a function of time. The normalised resolution versus time plots for all four gamma peaks are also shown. The resolution for the region of normal clean room temperature between the green markers (A-B) in Figure 4.15 was determined and this was compared to the resolution measured for the regions of increased clean room temperature (C-D) and decreased room temperature (E-F). The resolution for the regions (C-D) and (E-F) were normalised relative to the resolution obtained for the normal room temperature region. By definition this means that the normalised resolution for the normal room temperature is one with an error that can be determined from the unnormalised resolution value. The normalised results are presented in Table 4.11.

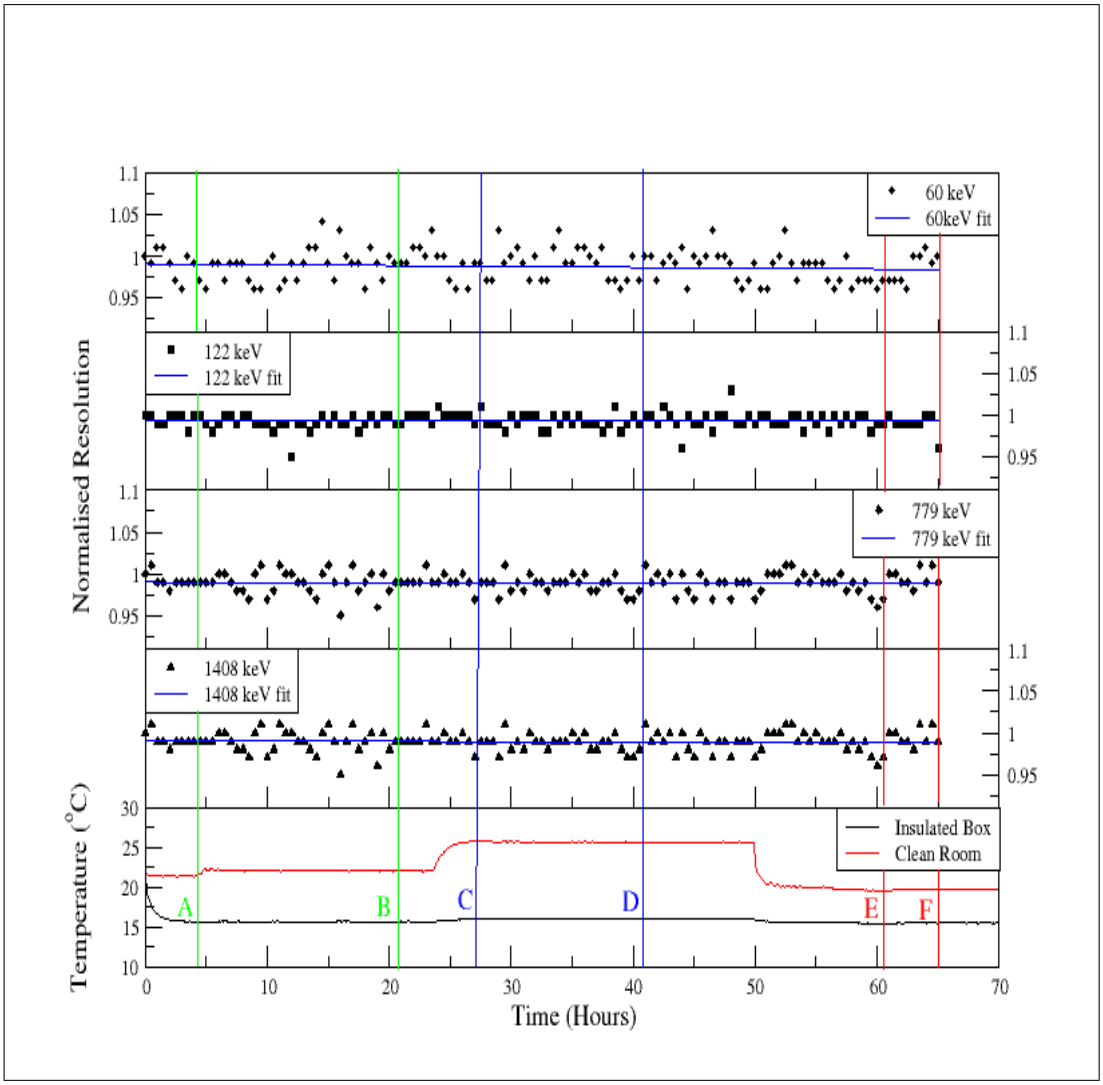

Figure 4.15: Temperature Variation plot for the Ortec Xcooler detector showing regions (A-B) which is the normal clean room temperature, (C-D) the region of increased temperature and (E-F) the region of decreased temperature. The normalised resolution versus time plots for the 60, 122, 779 and 1408 keV peaks are also presented. A least squares fit to the data points is shown for all the gamma peaks as a guide to the eye for the resolution stability over time. The oscillations present in the temperature plot are due to the temperature control system in the clean room. The error bars are typically in the order of 4% on the resolution versus time measurements.

	60 keV	122 keV	779 keV	1408 keV
Normal Room Temperature (22°C) (A-B)	1.000 ± 0.012	1.000 ± 0.012	1.000 ± 0.014	1.000 ± 0.011
Temperature increased by 4°C (C-D)(26°C)	0.987 ± 0.018	1.000 ± 0.017	1.000 ± 0.010	1.005 ± 0.012
Temperature decreased by 6°C (E-F)(20°C)	1.000 ± 0.018	1.000 ± 0.017	1.000 ± 0.001	1.000 ± 0.015

Table 4.11: The resolution of the increased (C-D) and decreased (E-F) temperature regions are normalised relative to the resolution obtained for the normal room temperature region. These results are presented for the 60, 122, 779 and 1408 keV gamma peaks for the Ortec Xcooler detector.

These results indicate that for the limited temperature variation encountered by the electronics in the the clean room, there is little or no measureable effect on the resolution measured within errors.

4.5.2 The Canberra Cryo-cycle Detector

Figure 4.16 shows the temperature of the clean room and the insulated box as a function of time. The normalised resolution versus time plots for all four gamma peaks are also shown. The resolution for the region of normal clean room temperature between the green markers (A-B) in Figure 4.16 was determined and this was compared to the resolution measured for the regions of increased clean room temperature (C-D) and decreased clean room temperature (E-F). The resolution for the regions (C-D) and (E-F) were normalised relative to the resolution obtained for the normal room temperature region (see section 4.5.1). The normalised results are presented in Table 4.12.

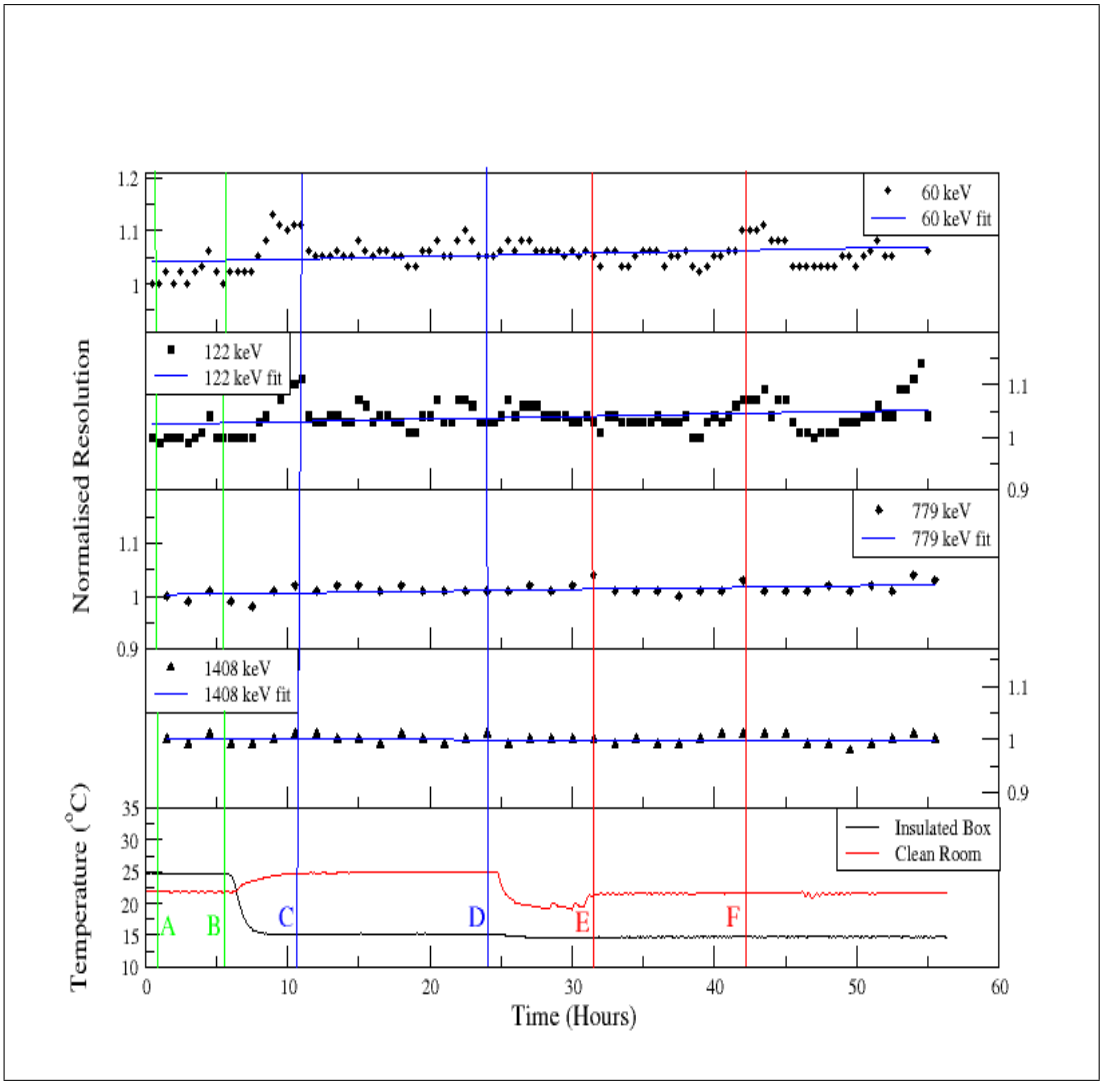

Figure 4.16: Temperature Variation plot for the Canberra Cryocycle detector showing regions (A-B) which is the normal clean room temperature, (C-D) the region of increased temperature and (E-F) the region of decreased temperature. The normalised resolution versus time plots for the 60, 122, 779 and 1408 keV peaks are also presented. It should be noted that there are fewer points for the higher energy peaks due to problems with peak fitting as discussed earlier (see section 3.5). A least squares fit to the data points is shown for all the gamma peaks as a guide to the eye for the resolution stability over time. The oscillations present in the temperature plot are due to the temperature control system in the clean room. The error bars are typically in the order of 4% on the resolution versus time measurements.

	60 keV	122 keV	779 keV	1408 keV
Normal Room Temperature (22°C) (A-B)	1.000 ± 0.031	1.000 ± 0.027	1.000 ± 0.007	1.000 ± 0.011
Temperature increased by 3°C (C-D)(25°C)	1.000 ± 0.034	1.000 ± 0.019	1.000 ± 0.0016	1.000 ± 0.012
Temperature decreased by 4°C (E-F)(21°C)	1.015 ± 0.034	1.013 ± 0.019	1.00 ± 0.01	1.000 ± 0.012

Table 4.12: The resolution of the increased (C-D) and decreased (E-F) temperature regions are normalised relative to the resolution obtained for the normal room temperature region. These results are presented for the 60, 122, 779 and 1408 keV gamma peaks for the Canberra cryocycle detector.

On examination of these results, one can again conclude that, over the limited temperature differences experienced by the electronics in this test, the resolution is not significantly affected by the this temperature difference ($\sim 7^o$C) and is certainly well within errors.

4.5.3 The Ortec Liquid Nitrogen Cooled Detector

Figure 4.17 shows the temperature of the clean room and the insulated box as a function of time. The normalised resolution versus time plots for all four gamma peaks are also shown. The resolution for the region of normal clean room temperature between the green markers (A-B) in Figure 4.17 was determined and this was compared to the resolution measured for the regions of increased clean room temperature (C-D) and decreased clean room temperature (E-F). The resolution for the regions (C-D) and (E-F) were normalised relative to the resolution obtained for the normal room temperature region (see section 4.5.1). The normalised results are presented in table 4.13. It should be noted that the clean room temperature recordings for this particular data set was less stable than usual.

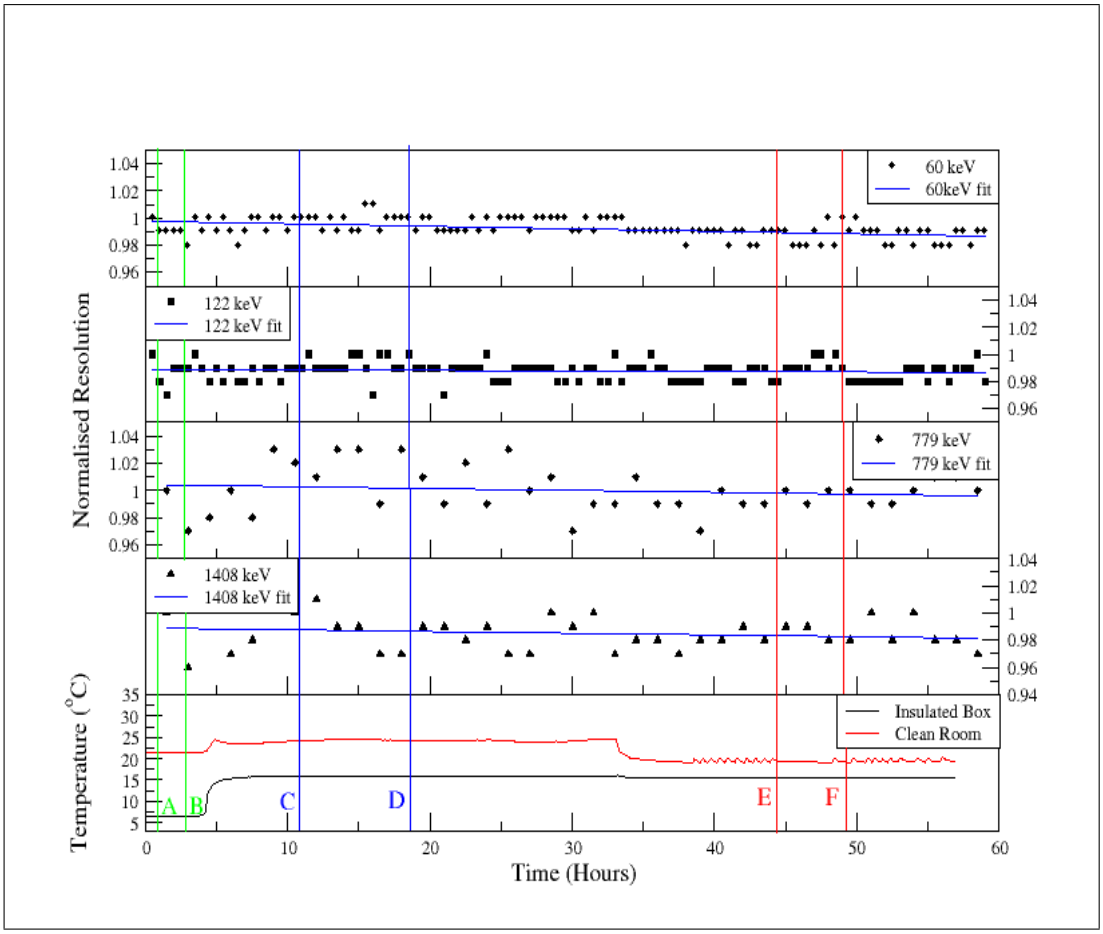

Figure 4.17: Temperature Variation plot for the Ortec liquid Nitrogen Detector showing regions (A-B) which is the normal clean room temperature, (C-D) the region of increased temperature and (E-F) the region of decreased temperature. The normalised resolution versus time plots for the 60, 122, 779 and 1408 keV peaks are also presented. It should be noted that there are fewer points for the higher energy peaks due to problems with peak fitting as discussed earlier (see section 3.5). A least squares fit to the data points is shown for all the gamma peaks as a guide to the eye for the resolution stability over time. The oscillations present in the temperature plot are due to the temperature control system in the clean room. The error bars are typically in the order of 3% on the resolution versus time measurements.

	60 keV	122 keV	779 keV	1408 keV
Normal Room Temperature (21.5°C) (A-B)	1.000 ± 0.012	1.000 ± 0.011	1.000 ± 0.014	1.000 ± 0.016
Temperature increased by 3°C (C-D)(24.5°C)	1.000 ± 0.016	1.000 ± 0.015	1.007 ± 0.015	1.00 ± 0.02
Temperature decreased by 6°C (E-F)(18.5°C)	1.012 ± 0.016	1.000 ± 0.015	1.014 ± 0.015	0.994 ± 0.019

Table 4.13: The resolution of the increased (C-D) and decreased (E-F) temperature regions are normalised relative to the resolution obtained for the normal room temperature region. These results are presented for the 60, 122, 779 and 1408 keV gamma peaks for the Ortec Liquid Nitrogen detector.

Once again it is clear that the temperature variation ($\sim 9\ ^{o}$C) encountered by the electronics had little effect on the resolution measured for this detector within error. The overall conclusion from these measurements is that within the limited temperature range used for the clean room operating temperature there was no obvious effect on the resolutions measured for any of the detectors used in the project.

4.6 The Canberra Cryo-cycle pump, switched on and off

The results of the Canberra detector with the cryo-pump switched on and off are as shown in Table 4.14. The temperature of the insulated box was held at 11°C during the data taking period. The resolution was normalised relative to the resolution values obtained for the pump-on data run with the error in this case being determined from the unnormalised standard deviation value on the resolution. The percent change in resolution between these two data sets is also presented in Table 4.14. This percent change is defined as the difference between the normalised resolution obtained for the pump on and the pump off, divided by the normalised resolution of the pump on.

No. of Run	60 keV	122 keV	779 keV	1408 keV	Temp(^{o}C)
Pump On	1.000 ± 0.022	1.000 ± 0.022	1.000 ± 0.011	1.000 ± 0.008	11
Pump Off	0.938 ± 0.021	0.947 ± 0.021	0.997 ± 0.015	0.998 ± 0.011	11.5
% Change in Resolution	6.2 ± 3.0	5.3 ± 3.0	0.3 ± 1.8	0.2 ± 1.3	-

Table 4.14: Results of the normalised resolution relative to the pump on value for each of the 4 gamma peaks (60, 122, 779 and 1408 keV) with the cryo-pump switched on and off. The percent change between these two data sets is also presented (see text for details).

These results show that the pump appears to show an improvement of up to $\sim 6\%$ in resolution at the lower end of the energy range but no effect at the higher energies. These results are in agreement with the manufacturers specifications [Can] in which they claim that these detectors are guaranteed to exhibit virtually no resolution loss with the cryocooler in operation.

4.7 Absolute and Relative Efficiency measurements

The absolute and relative efficiencies for the Ortec Xcooler detector, the Canberra Cryo-cycle detector and the Ortec Liquid Nitrogen detector are presented in section 4.7.1, 4.7.2 and 4.7.3, respectively. These measurements were taken with a ^{60}Co point source (ref no. LW995) whose activity on a specific date (01/09/03) was quoted as being accurate to 3%.

4.7.1 The Ortec Xcooler Detector

In this case the source was placed 24.5 cm from the detector face (taking account of the endcap to crystal distance and the endcap thickness). The data was gathered for 600 seconds and the spectrum was analysed to find the area of the 1333 keV gamma peak using the AF1 fitting function in gf3. The parameters used in the calculation of the efficiency are presented in Table 4.15. The formulae used to calculate the absolute and relative efficiency are given by equations 1.4 and 1.5, respectively (see section 1.4.4).

Date of Spectrum Run	09/09/09
Activity of Source	1.76 $\times 10^5$ Bq
Live Time	600 seconds
Area	82409(294) counts
$\varepsilon_{absoluteNaI}$	1.2×10^{-3}
$\varepsilon_{relativeGe}$ as quoted by Manufacturer	60%
$\varepsilon_{relativeGe}$ measured	65 ± 3%
$\varepsilon_{absoluteGe}$ measured	$7.80 \times 10^{-4} \pm 0.23 \times 10^{-4}$

Table 4.15: Parameters used to calculate the efficiency of the Ortec Xcooler Detector. Also presents the values measured for the absolute and relative efficiency for the detector.

4.7.2 The Canberra Cryocycle Detector

When taking the ^{60}Co spectrum for the efficiency test for this detector, the source was placed 245 mm from the front face of the detector (taking account of the fact that the endcap to crystal distance was 4.5 mm and the endcap thickness was 0.5 mm). The efficiency was calculated using the parameters presented in Table 4.16. Once again, the formulae used to calculate the absolute and relative efficieny are given by equations 1.4 and 1.5, respectively (see section 1.4.4).

Date of Spectrum Run	07/10/09
Activity of Source	1.75 $\times 10^5$ Bq
Live Time	600 seconds
Area	25151(159) counts
$\varepsilon_{absoluteNaI}$	1.2×10^{-3}
$\varepsilon_{relativeGe}$ as quoted by Manufacturer	23.3%
$\varepsilon_{relativeGe}$ measured	19.9 ± 3.0%
$\varepsilon_{absoluteGe}$ measured	$2.29 \times 10^{-4} \pm 0.07 \times 10^{-4}$

Table 4.16: Parameters used to calculate the efficiency of the Canberra Cryocycle Detector. Also presents the values measured for the absolute and relative efficiency for the detector.

4.7.3 The Ortec Liquid Nitrogen Detector

Finally, the absolute efficiency was calculated for the LN2 Ortec detector in which the source was placed 246.5 mm from the front face of the detector (endcap to crystal distance is 3 mm and the endcap thickness is 0.5 mm). The efficiency is calculated using the parameters presented in Table 4.17. As before the absolute and relative efficiencies are given by equations 1.4 and 1.5, respectively (see section 1.4.4).

Date of Spectrum Run	27/10/09
Activity of Source	1.73 $\times 10^5$ Bq
Live Time	600 seconds
Area	17032(132) counts
$\varepsilon_{absoluteNaI}$	1.2×10^{-3}
$\varepsilon_{relativeGe}$ as quoted by Manufacturer	10%
$\varepsilon_{relativeGe}$ measured	$14 \pm 3\%$
$\varepsilon_{absoluteGe}$ measured	$1.68 \times 10^{-4} \pm 0.05 \times 10^{-4}$

Table 4.17: Parameters used to calculate the efficiency of the Ortec Liquid Nitrogen Detector. Also presents the values measured for the absolute and relative efficiency for the detector.

The results from all detectors agree within errors with the relative efficiency values quoted by the manufacturers.

4.8 Summary Table of Results

No. of Test	Description	LCR	LCR	LCR	LCR	HCR	HCR	HCR	HCR
		60 keV	122 keV	779 keV	1408 keV	60 keV	122 keV	779 keV	1408 keV
Test 1	Resolution versus Temperature								
	Ortec Xcooler Detector	No	No	No	No	No	No	Yes	Yes
	Canberra Cryocycle Detector	Yes	Yes	No	No	No	No	No	No
	Ortec Ln2 Detector	No	No	No	No	No	No	No	No
Test 2	Fluctuation in Clean Room Temperature								
	Ortec Xcooler Detector	No	No	No	No				
	Canberra Cryocycle Detector	No	No	No	No				
Test 3	Temperature Variation of Electronics								
	Ortec Xcooler Detector	No	No	No	No				
	Canberra Cryocycle Detector	No	No	No	No				
	Ortec Ln2 Detector	No	No	No	No				
Test 4	Pump switched on and off								
	Canberra Cryocycle Detector	Yes	Yes	No	No				

Table 4.18: Summary Table of Results where No = Not Significant, Yes = Significant, LCR = Low Count Rate and HCR = High Count Rate.

Chapter 5

Final Conclusions and Future Work

The prime aim of this thesis was to investigate how the resolution of selected gamma peaks varies as a function of the ambient room temperature in which the detectors were housed. Returning to this question posed at the beginning of this project, it is now possible to state that in general these findings reveal that each of the three detectors investigated displayed slightly different behaviour. Section 5.1 discusses these differences in more detail. In section 5.2 of this chapter, many interesting options are suggested as possibilities for future work in relation to this project.

5.1 Final Conclusions

5.1.1 The Ortec Xcooler Detector

The first detector to be tested was the Ortec Xcooler detector. This was a p-type HPGe coaxial detector with a relative efficiency of $\sim 60\%$. This detector was cooled using an electro/mechanical cooler. On examination of the low count rate data, it is apparent that there is little evidence for any significant changes in the resolution for any of the four peaks measured as a function of ambient room temperature. However, the data obtained at high count rates for this detector indicate that there is no statistically significant effect for the low energy gamma rays. Interestingly, for the higher energy gamma rays (e.g. the 779 keV and the 1408 keV transitions) analysed there is a small but statistically significant change in resolution as a function of ambient room temperature. This is found to be in the region of 0.9(4)% and 4.1(7)% for a temperature difference of $\sim 17^{o}$C for the 779 keV and the 1408 keV, respectively.

5.1.2 The Canberra Cryocycle Detector

The second detector used in this project was the Canberra cryocycle detector. This was an n-type BEGE detector with a relative efficiency of $\sim 23.3\%$. This was cooled using a hybrid electro mechanical/liquid nitrogen cooling system. The pump of this cooling system could be switched off for an appreciable amount of time, which meant that tests could be carried out to measure the effect that this pump has on the resolution. After careful examination of the low count rate data from this detector, the data suggests that there is an improvement in resolution with increasing ambient room temperature, for the low energy gamma peaks ($\sim 5\%$ over a temperature range $\sim 19^{o}$C), but with little improvement evident for the high energy gamma ray transitions. Due to the lack of data points in the high count rate plot it was difficult to determine whether or not there was any significant effect on the resolution. There is very weak evidence for a slight improvement in resolution for the 60 keV and the 122 keV gamma rays. However, it is clear that further measurements would be needed to confirm this suggestion.

Tests were carried out with the cryo-pump turned off. Results for the resolution were compared with results for resolution for the same temperature with the pump turned on. There was a 6.2(30)% improvement in the resolution of the 60 keV peak and a 5.3(30)% improvement for the 122 keV, but there was no obvious change in the resolution at higher energies. These results are in agreement with the manufacturers specifications [Can] in which they claim that these detectors are guaranteed to exhibit virtually no resolution loss with the cryocooler in operation.

5.1.3 The Liquid Nitrogen Cooled Detector

This was the final detector to be analysed during this project. This was an n-type HPGe coaxial detector with a relative efficiency of $\sim 10\%$. This detector was cooled using the traditional Liquid Nitrogen method. It is apparent that for both the low and high count rates for this detector, there are no statistically significant changes in the resolution for any of the four gamma ray peaks analysed as a function of ambient room temperature.

5.1.4 Electronics Temperature Variation Tests

This batch of tests set out to determine whether the temperature variations of the room in which the electronics were situated would have an effect on the resolution determined for each detector. These findings suggest that over the temperature range chosen ($\pm$ 5 ^{o}C from the standard operating temperature used for all tests), this variation had essentially no effect on the resolution measured. One can conclude therefore that temperature fluctuations of the electronics environment of $\pm$ 5 ^{o}C have no effect on the resolution of the detector. It would clearly be interesting to perform further measurements to investigate a somewhat larger temperature range from the standard operating temperature, to determine if this conclusion holds true for more extreme temperature variations. These tests also confirm that the small temperature fluctuations witnessed in the clean room temperature would have no influence on the resolution determined.

5.2 Future Work

Following the investigations discussed in this thesis there are a number of projects or further investigations that could be carried out in the future that could be a welcome addition to the results of this project.

5.2.1 Verification of Results

Both the Ortec Xcooler detector and the Canberra Cryocycle detector exhibited statistically significant changes in the values obtained for resolution as a function of ambient room temperature. In particular, the high count rate results for the resolution of the high energy gamma rays increased as a function of temperature for the Ortec Xcooler detector, while the opposite was true for the Canberra cryocycle detector, in which the low count rate results obtained for the resolution of the low energy gamma rays decreased as a function of temperature. Also, there is very weak evidence to suggest that there is an improvement in resolution of the high count rate low energy gamma rays. Further investigations need to be carried out in order to confirm this. In order to verify that these conclusions holds true in all cases, it would be of benefit to carry out further experimentation, concentrating on these two detectors specifically. One could carry out analysis on other gamma peaks in the energy regions specified for each detector. An increased number of data collection runs could be made for smaller temperature intervals of values within the temperature range of $5^oC < T < 30^oC$. Perhaps further statistical analysis of the data could also be carried out to determine the statistical significance of no temperature dependance and deviation of the slope from the straight line (angle Θ).

5.2.2 Reversal of apparatus setup

This project involved determining the resolution of a detector for a given temperature in the insulated box, while the temperature of the electronics was held at a stable temperature ($\pm$ 0.2^oC) in the clean room. An investigation could be carried out with the setup reversed, i.e. the electronics could be placed inside the insulated box, with the detector located in the clean room. It could be established if a change in the temperature of the electronics over a larger temperature range than that investigated in the present work would have had an effect. This would be useful if the electronics is also subject to uncontrolled environmental conditions at Sellafield. It is interesting to note that the amplifier used in this project (Ortec model 572) has a temperature

instability quoted as follows: Gain $\leq 0.0075\%/^{o}$C, 0 to 50^{o}C [Orte], whilst the bias supply used (Model number 659) is quoted as having a temperature sensitivity of output voltage of $\pm$ 0.08%/^{o}C through 10 ^{o}C to 50^{o}C operating range [Ortf].

5.2.3 PT 1000 signal

At the outset of this experiment one of the goals was to measure the resolution of the gamma peaks as a function of crystal temperature. The temperature of the crystal was to be monitored using the PT1000 signal. This was not possible due to problems in accessing the PT1000 signal for all detectors used. If this aspect is to be pursued in the future, then it would require the use of detectors that have easy read out mechanisms for the crystal temperature.

5.2.4 Centroid Monitoring and Analysis of further gamma ray peaks

Further data analysis, such as monitoring the centroid position or determining the resolution for more gamma peaks than those selected for analysis in this project could be carried out. The fitting of all peaks, using the gf3 analysis programme, was carried out manually, which was a very labour intensive and time consuming task. It would be of interest to attempt to determine a method of automatically extracting the required information, allowing more peaks in the spectrum to be analysed. The centroid position was not extracted except for a couple of cases. Some of these showed shifts in position, hence it would be useful to re-analyse the data to look at how much of a problem these shifts are, as over time since they can obviously affect the resolution extracted and hence presumably the ability of an automatic peak monitoring program to identify peaks in a spectrum. An attempt was made at a late stage of the project to get the GEANIE software to automatically fit the FWHM to a range of gamma ray peaks in a spectrum but this was not successful in the time available.

5.2.5 More detectors for Investigation

Originally, at the beginning of this project it was suggested that up to seven detectors would be tested over the duration of this project. Due to time constraints and delivery problems this was limited to three detectors. A fourth was delivered, but unfortunately had to be returned due to damage that occurred in transit. It would clearly have been interesting to carry out tests on more electro/mechanically cooled detectors than we were able to manage in the current project.

List of Figures

List of Tables

Appendix A

Photographs of the Final Experimental Set-up

The following presents photographs of the Final experimental set-up for each of the detectors. Photographs of the Heater matrix, fan and NIM modules used are also presented.

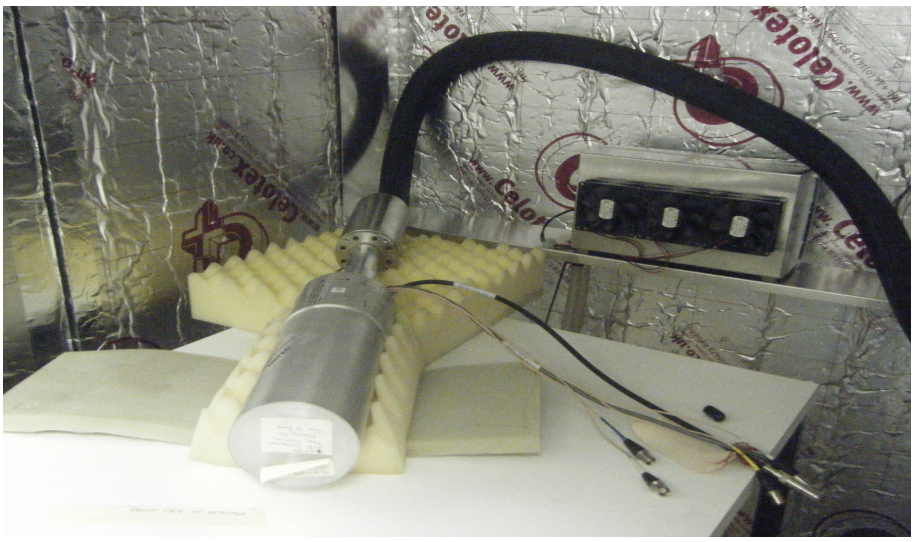

Figure A.1: Photograph of the Ortec Xcooler Detector placed in the insulated box.

Figure A.2: Photograph of the Canberra Cryo-cycle Detector placed in the insulated box.

Figure A.3: Photograph of the Ortec Liquid Nitrogen Detector placed in the insulated box. Also shown is the stand for the sources. Note the position of the Tinytag data logger in relation to the detector.

Figure A.4: Heater/Pump used to heat the Insulated Box.

Figure A.5: Fan placed at back end of Insulated Box to circulate the heat.

Figure A.6: Photograph of the NIM modules used over the duration of this project.

Appendix B

Tiny Tag Temperature Data Recordings.

B.1 The Ortec Xcooler Detector – Low count rate data

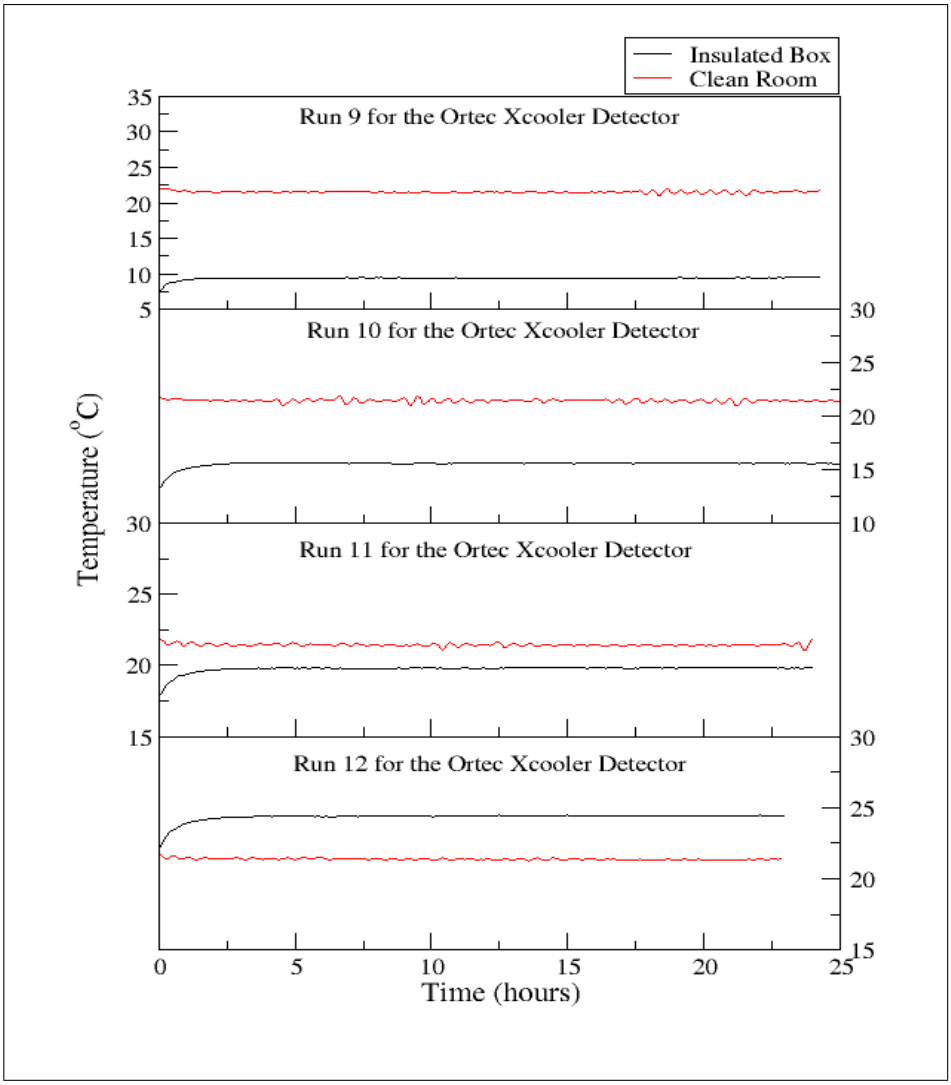

Figure B.1: The temperature recordings for the low count rate data of the Ortec Xcooler detector. The oscillations present in these plots are due to the temperature control system in the clean room.

B.2 The Ortec Xcooler Detector – High Count rate data

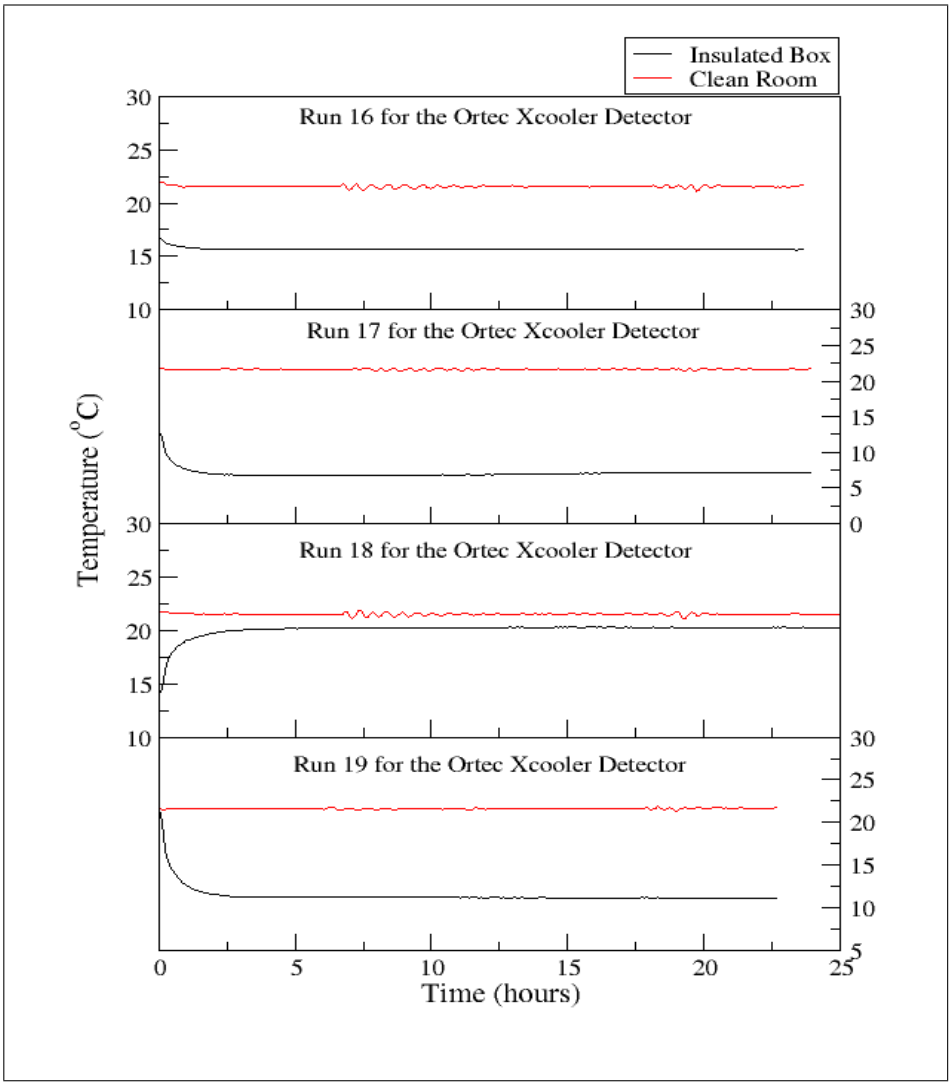

Figure B.2: The temperature recordings for the high count rate data of the Ortec Xcooler detector. The oscillations present in these plots are due to the temperature control system in the clean room.

B.3 The Canberra Cryocycle Detector – Low count rate data

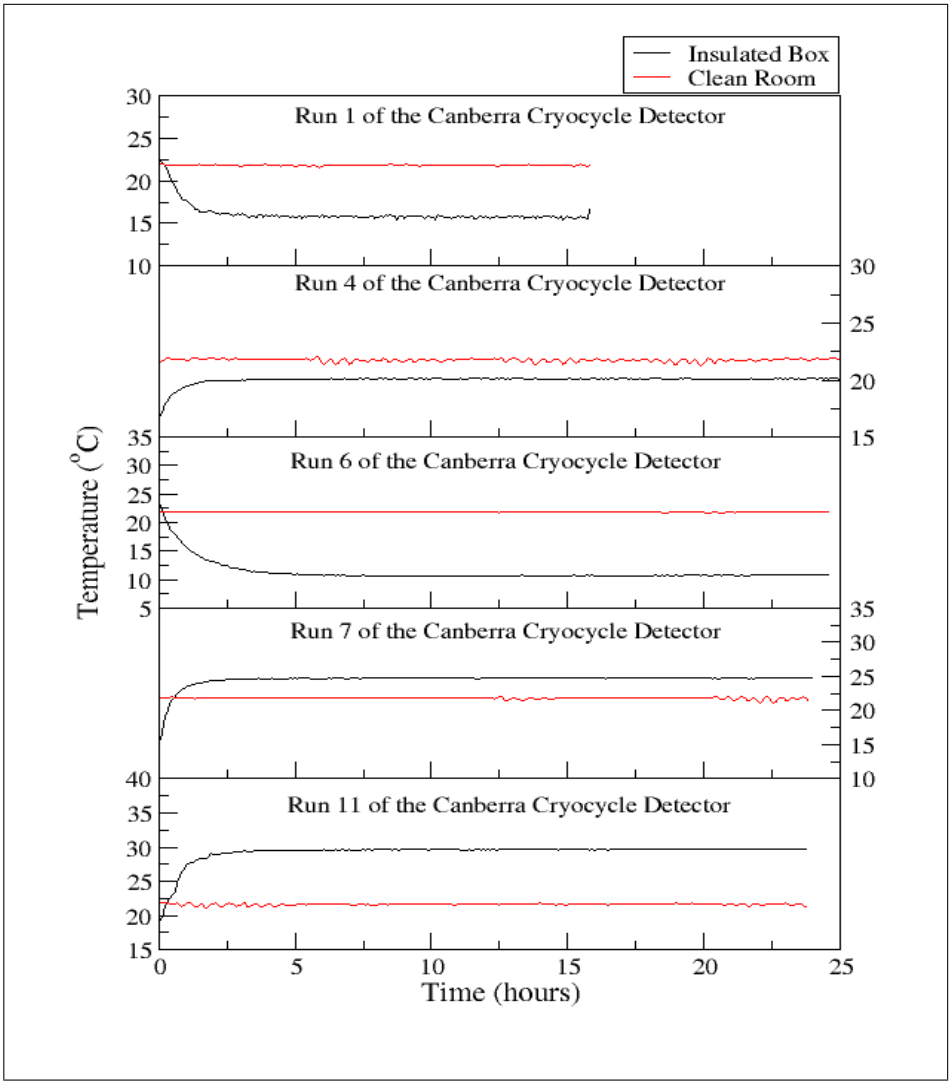

Figure B.3: The temperature recordings for the low count rate data of the Canberra Cryocycle detector. The oscillations present in these plots are due to the temperature control system in the clean room.

B.4 The Canberra Cryocycle Detector – Pump switched on and off data

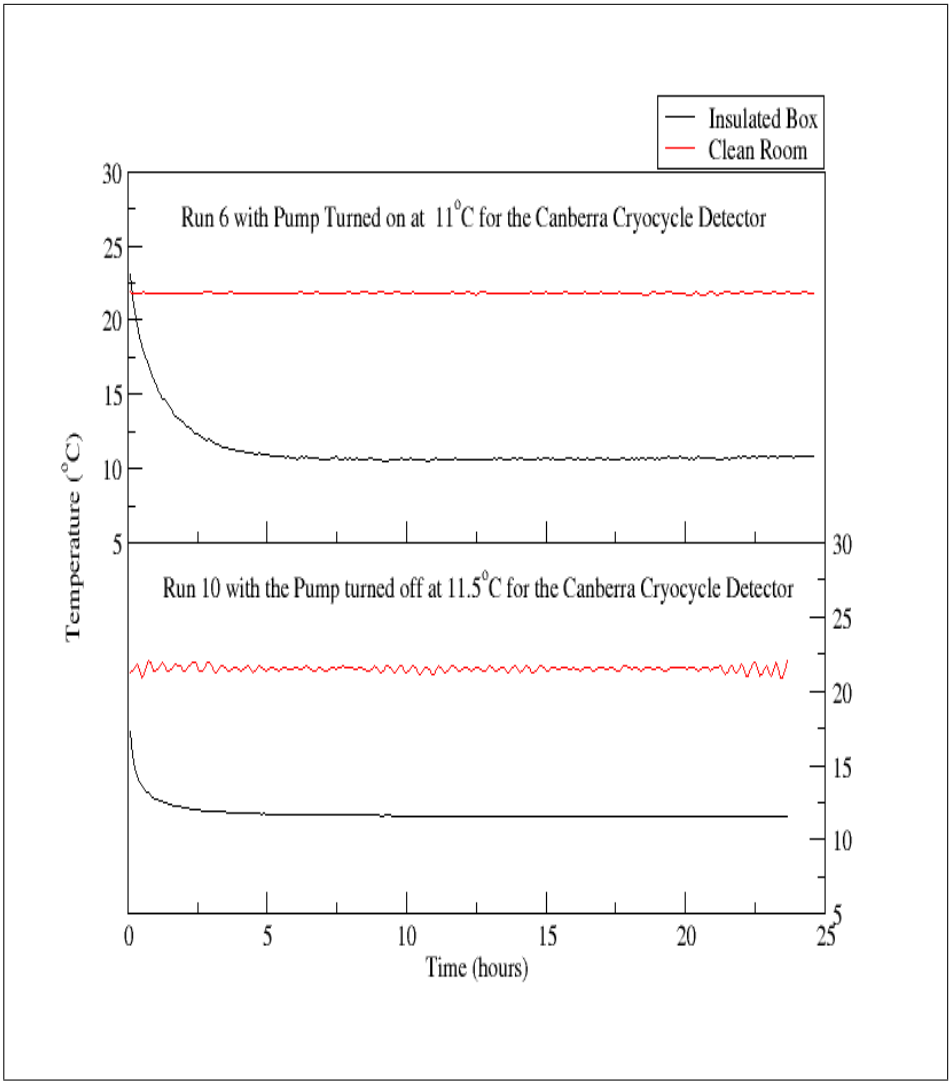

Figure B.4: The temperature recordings for the comparison of the Pump on (run 6) versus Pump off (run 10) for the Canberra Cryocycle detector. The oscillations present in these plots are due to the temperature control system in the clean room.

B.5 The Canberra Cryocycle Detector – High Count rate data

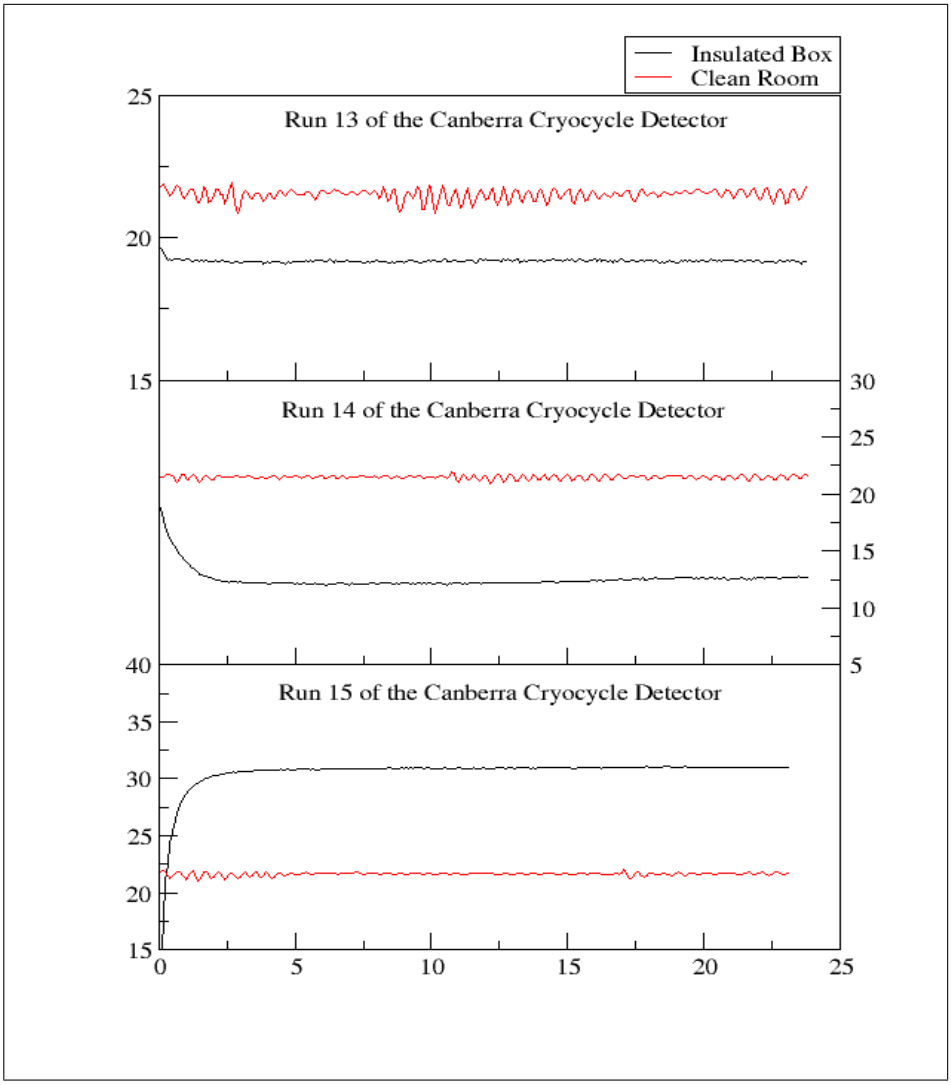

Figure B.5: The temperature recordings for the high count rate data of the Canberra Cryocycle detector. The oscillations present in these plots are due to the temperature control system in the clean room.

B.6 The Ortec Liquid Nitrogen Detector – Low count rate data

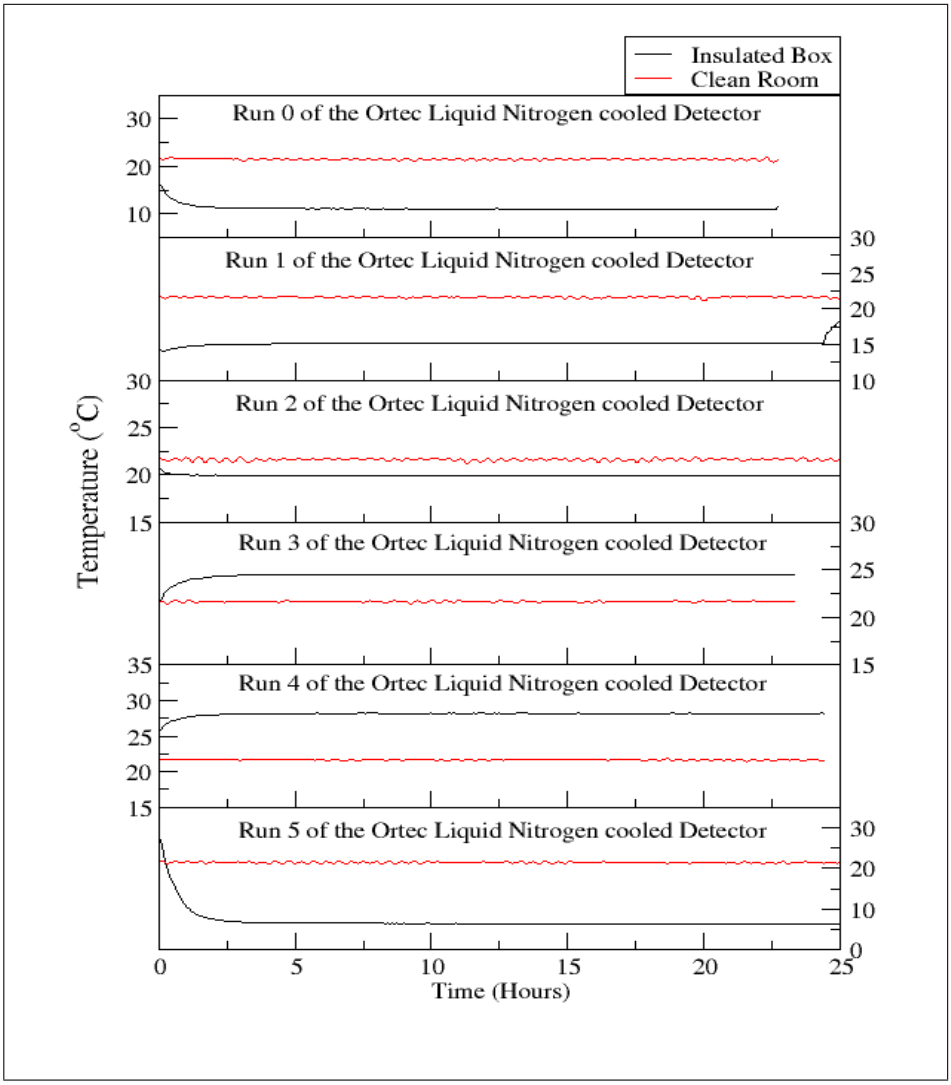

Figure B.6: The temperature recordings for the low count rate data of the Ortec Liquid Nitrogen cooled detector. The oscillations present in these plots are due to the temperature control system in the clean room.

B.7 The Ortec Liquid Nitrogen Detector – High Count rate data

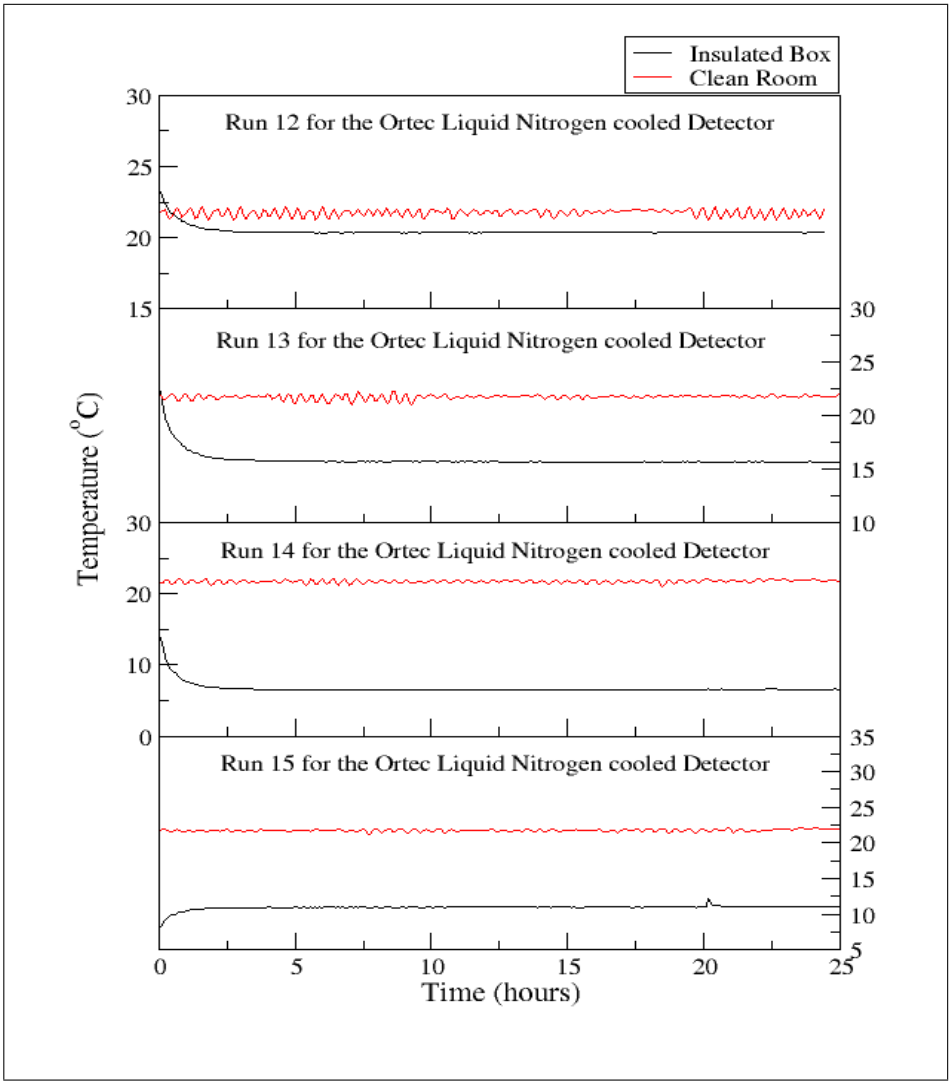

Figure B.7: The temperature recordings for the high count rate data of the Ortec Liquid Nitrogen cooled detector. The oscillations present in these plots are due to the temperature control system in the clean room.

Bibliography

[Can] Canberra. *Cryo-cycle Cryostat*. Canberra Industries, 800 Research Parkway, Meriden, USA. CryoCycleCryostat-DET-ss.pdf.

[Can03] Canberra. *Germanium Detectors Manual*. Canberra Industries, 800 Research Parkway, Meriden, USA, 2003. Chapter 2, pp19-20.

[GDL] Gemini Data Loggers. Temperature data loggers. http://www.geminidataloggers.com/file/loggers$_v ariant/datasheet/tgu$ − 4017.*pdf*.

[JL08] John Lilley. *Nuclear Physics, Principles and Applications*. Wiley, Chichester, West Sussex, England, March 2008. Chapter 6, pp158 - 159, [6.4].

[Kno00a] Glenn F. Knoll. *Radiation Detection and Measurement*. Wiley, United States of America, third edition edition, 2000. Chapter 17, pp611.

[Kno00b] Glenn F. Knoll. *Radiation Detection and Measurement*. Wiley, United States of America, third edition edition, 2000. Chapter 12, pp406-407.

[Kno00c] Glenn F. Knoll. *Radiation Detection and Measurement*. Wiley, United States of America, third edition edition, 2000. Chapter 12, pp408.

[Kno00d] Glenn F. Knoll. *Radiation Detection and Measurement*. Wiley, United States of America, third edition edition, 2000. Chapter 12, pp416-418.

[Kno00e] Glenn F. Knoll. *Radiation Detection and Measurement*. Wiley, United States of America, third edition edition, 2000. Chapter 12, pp449-450.

[Kra88a] Kenneth S. Krane. *Introductory Nuclear Physics*. Wiley, Canada, 1988. Chapter 7, pp216-217, [7.4].

[Kra88b] Kenneth S. Krane. *Introductory Nuclear Physics*. Wiley, Canada, 1988. Chapter 7, pp225, [7.6].

[Leo94a] W. R. Leo. *Techniques for Nuclear and Particle Physics Experiments.* Springer - Verlag, New York, third edition edition, 1994. Chapter 10, pp227, [10.3.3].

[Leo94b] W. R. Leo. *Techniques for Nuclear and Particle Physics Experiments.* Springer - Verlag, New York, third edition edition, 1994. Chapter 10, pp240, [10.7.1].

[Leo94c] W. R. Leo. *Techniques for Nuclear and Particle Physics Experiments.* Springer - Verlag, New York, third edition edition, 1994. Chapter 5, pp117-118, [5.3].

[Leo94d] W. R. Leo. *Techniques for Nuclear and Particle Physics Experiments.* Springer - Verlag, New York, third edition edition, 1994. Chapter 5, pp243, [10.9.1].

[NI] National Instruments. N.i. labview. http://www.ni.com/labview/.

[Ome] Omega. Omega engineering technical reference. http://www.omega.co.uk/prodinfo/pt100.html.

[Orta] Ortec. *GEM Series Coaxial HPGe Detector Product Configuration Guide.* Oakridge, TN, USA. GEM.pdf.

[Ortb] Ortec. *GMX Series Coaxial HPGe Detector Product Configuration Guide.* Oakridge, TN, USA. GMX.pdf.

[Ortc] Ortec. *Maestro - 32 v5.35.01, MCA Emulation Software.* Oakridge, TN, USA. A65-B52-MAESTRO-32-MCA-Emulation-Software.pdf.

[Ortd] Ortec. *Maestro - 32 v6.08, MCA Emulation Software.* Oakridge, TN, USA. A65-B52-MAESTRO-32-MCA-Emulation-Software.pdf.

[Orte] Ortec. *Model 572 Spectroscopy Amplifier and Pile-up Rejector Operating and Service Manual.* Oakridge, TN, USA. section 2.1, pp 4.

[Ortf] Ortec. *Ortec, 5-kV Detector Bias Supply.* Oakridge, TN, USA. 659-5-kV-Detector-Bias-Supply[1].pdf.

[Rad] D.C. Radford. Radware. http://radware.phy.ornl.gov/main.html.

[Val] U Value. U-value. http://www.uvalue.co.uk/.